Annual report on the multi use social and economic data bank, vol. **92**, 2015

Land-Use/Land-Cover Changes in Major Asian and African Cities

Yuji MURAYAMA, Ronald C. ESTOQUE, Shyamantha SUBASINGHE, Hao HOU, and Hao GONG

Division of Spatial Information Science
Graduate School of Life and Environmental Sciences
University of Tsukuba, Japan

Keywords:
Asia, Africa, GIS, land-use, land-cover, megacities, remote sensing

1. Introduction

The surface of the earth is undergoing rapid land-use/land-cover (LULC) changes due to various socioeconomic activities and natural phenomena. These changes are occurring in a range of spatial scales from local to global and at temporal frequencies of days to millennia (Townshend et al. 1991). Understanding the process and pattern of LULC changes over time and space remains one of the challenging exercises not only in the field of land-change science but also in the field of geospatial sciences.

Remote sensing technology has a long history of supporting LULC map development, even before the launch of the first Landsat platform in 1972 (Sohl & Sleeter 2011). Aerial photography served as a primary source of information for LULC mapping prior to the availability of satellite imagery, and still remains an important source (Akbari et al. 2003). In recent years, low to medium spatial resolution (multispectral: 5~250 m; e.g. MODIS, ASTER, ALOS, SPOT, LANDSAT) and high spatial resolution (multispectral: 0.6~5 m; e.g. IKONOS, QuickBird, GeoEye) satellite imageries have been used in LULC change-related studies. Remote sensing satellite imageries, combined with a geographical information system (GIS), provide more efficiency in LULC mapping and change detection and modeling. Satellite remote sensing is a relatively inexpensive and efficient method of acquiring up-to-date information about the LULC of a large geographical area, compared to the traditional aerial photogrammetry and land surveys. It is also one of the practical methods used for obtaining data for inaccessible regions.

The terms “land use” and “land cover” are often used interchangeably in literature and daily practice. The term “land cover” basically explains the cover of features prevailing on the surface of the earth. Forest cover, glacier cover, lakes, wetlands, agriculture, and water can be considered as land cover. Land cover is defined as the immediate surface, including biota, soil, topography,

surface and ground water, and human structure (mainly built-up) (Lambin et al. 2006), while the term "land use" indicates how human beings utilize or associate the landscape of any area. In other words, a parcel of land (land cover) can be utilized for or associated with activities such as forestry, animal husbandry and farmland, etc. In this context, land use is defined as the purpose for which humans exploit the land cover. It involves both the manner in which biophysical attributes of the land are manipulated and the intent underlying that manipulation (Lambin et al. 2006). Natural and physical scientists are more interested in land-cover changes, while geographers, anthropologists and planners focus more on land-use changes (Turner & Meyer 1994). The less deviation between land use and land cover has created a common platform for the discussion of LULC change.

The knowledge of LULC is important in the management of the earth's resources in general, and in landscape and urban planning in particular. LULC changes are so pervasive that, when aggregated globally, they significantly affect key aspects of earth system functioning (Lambin et al. 2001). LULC changes are usually examined from various perspectives in order to identify the drivers of such changes and their processes and consequences at different spatial and temporal scales. The new era of LULC mapping started after NASA's launch of the Earth Resource Technology Satellite (later renamed Landsat) in July 1972. Landsat still remains as a leading satellite data provider globally. In the context of LULC classification, the 1976 publication "A Land Use and Land Cover Classification System for Use with Remote Sensor Data" provides a classification system that defines LULC categories that can be derived from remote sensing satellite imageries (Anderson 1976). Over the years, many satellite data sources and classification systems have emerged, parallel to the advancement of satellite remote sensing technology. Indeed, "the ever-expanding constellation of satellite platforms has acquired thousands of trillions of bytes of data invaluable for planning and land management applications" (Rogan & Chen 2004, p. 304). The early applications of remote sensing technology were largely experimental, but soon expanded in the field of land-use science (Aspinall 2006; Müller & Munroe 2014), which is also known as land-change science (Gutman et al. 2004; Turner et al. 2007) and land-system science (Reenberg 2009; Verburg et al. 2013).

The recent advancement of remote sensing technology has, in one way or another, helped researchers investigate the pattern and process of LULC change in various contexts, such as in the contexts of vegetation analysis (Goodchild 1994; Stow et al. 2004; Anderson et al. 2010; Hüttich et al. 2011; Yang et al. 2012; Smith et al. 2014), urban/suburban studies (Chan et al. 2001; Seto et al. 2011; Benediktsson et al. 2003; Chen et al. 2006; Mundia, Aniya & Murayama 2011; Thapa & Murayama 2008; Estoque & Murayama 2013a; Bagan & Yamagata 2014), wetland monitoring (Chopra et al. 2001; Phinn et al. 2000; Tong et al. 2014), crop mapping and monitoring (Moran et al. 1997; Fang 1998; Ferencz et al. 2004; Bellvert et al. 2013) and ecosystem services (Nelson et al. 2009; Polasky et al. 2011; Estoque & Murayama 2012, 2013b). Using satellite remote sensing and other ancillary data, future LULC changes can also be projected (Estoque & Murayama 2012; Thapa & Murayama 2012a, 2012b; Vimal et al. 2012; Arsanjani et al. 2013; Moghadam & Helbich 2013).

In the last decade, several LULC databases were also established. For example, in 2010, China launched the GlobeLand30 mapping project, and produced a 30 m global land-cover data product with 10 classes for the years 2000 and 2010 (http://www.globallandcover.com). On the other hand, the Atlas of Urban Expansion (Angel et al. 2012) provides a geographic and quantitative dimension of LULC changes in the major cities of the world. In addition, the Lincoln Institute of Land Policy (http://www.lincolninst.edu) also provides an urban LULC

database for 3,646 cities. Recently, the Food and Agriculture Organization (FAO) of the United Nations (UN) introduced a LULC database called the Global Land Cover-SHARE for the year 2014 under the Global Land Cover Network (GLCN) (http://www.glcn.org). About 14 years ago (2000), the Joint Research Centre of the European Commission developed the Global Land Cover 2000 database (http://bioval.jrc.ec.europa.eu). Furthermore, the European Space Agency (ESA) has also established a global LULC map database (http://due.esrin.esa.int/globcover) for the years 2005 and 2009. The Socioeconomic Data and Applications Center (SEDAC) of NASA (http://sedac.ciesin.columbia.edu) is another database that provides verification of LULC data at the regional level.

The recent expansion of urban areas substantially altered the LULC pattern of the world. According to the UN statistics for the year 2014, 54% of the world's total population live in urban areas (UN 2014). If the current trends continue, the world's urban population is expected to increase up to 66% by 2050 (UN 2014). In 1950, the world's urban population was 30% (UN 2014). These statistics show that the growth of urban population has been very rapid in the past six decades. According to the UN, "several decades ago most of the world's largest urban agglomerations were found in the more developed regions, but today's large cities are concentrated in the global south. The fastest growing urban agglomerations are medium-sized cities and cities with less than 1 million inhabitants located in Asia and Africa" (UN 2014, p. 1). Furthermore, LULC changes in the unplanned urban areas of the developing countries are also faster than in the developed countries (Haregeweyn et al. 2012).

Today, various studies focus on the urbanization patterns in the developing countries, especially in the Asian and African regions (Estoque & Murayama 2011; Mundia et al. 2011; Yamashita 2011; Thapa & Murayama 2012a, 2012b; Dadras et al. 2014; Estoque et al. 2014). Analyses and projections of urbanization patterns can help with the assessment of ecosystem changes and their environmental implications at various temporal and spatial scales (Lambin & Ehrlich 1997). Additionally, the time-space relationship is also important for understanding the dynamic process of urban growth and LULC changes (Thapa & Murayama 2012a). We recognize that these types of analyses are important for landscape and urban planning toward sustainable urban development. However, these analyses can only be done if LULC data are available.

In most Asian and African cities, however, the availability of multi-temporal and spatially consistent LULC maps is still limited. Remote sensing technology supports LULC mapping and spatiotemporal change detection in different landscapes, including urban areas. It has been argued that in the context of remote sensing and urban studies, the Landsat series are one of the most important sources of satellite data for studying urban growth. The start of the Landsat series, i.e. 1972, is parallel to the rapid urban expansion in the Asian and African regions, i.e. approximately after the year 1970. Thus, Landsat imageries might help in the study of urban growth and LULC changes in the Asian and African cities.

The primary objective of this project is to establish a database of LULC maps derived from remote sensing satellite imageries (Landsat imageries) for major Asian and African cities. It also aims to detect the changes in the landscape of these cities and examine how the spatial structure of each city has changed over the years (2000–2014). The remainder of this report is structured as follows: Chapter 2 describes some of the available satellite data and their characteristics; Chapter 3 provides an overview of LULC classification methods and describes the study areas and data processing methodologies; Chapter 4 presents the classification and change detection results for each study area; and Chapter 5 gives a brief summary.

2. Data availability

Remote sensing satellite imageries are the primary source of data for LULC mapping and change detection. Remote sensing can be categorized into two types: active remote sensing and passive remote sensing.

An active sensor is a radar instrument used for measuring signals transmitted by the sensor that were reflected, refracted or scattered by the earth's surface or its atmosphere (http://www.nasa.gov). RADAR and LiDAR are examples of active remote sensing. The time delay between emission and return is measured, establishing the location, speed and direction of an object (http://www.nasa.gov). Active remote sensing depends on airborne remote sensing systems, which acquire data with specific needs and fly when the weather conditions are optimal. Users can choose the wavelength bands, area, season and other parameters according to their needs. However, active remote sensors do not offer continuous data sets since they only get data by order. Also, users need to consider the costs and time delay in the ordering process when choosing active remote sensing data.

On the other hand, a passive sensor is a microwave instrument designed to receive and to measure natural emissions produced by constituents of the earth's surface and its atmosphere (http://www.nasa.gov). Reflected sunlight is the most common source of radiation measured by passive sensors. Examples of passive remote sensors include film photography, infrared and radiometers. Nowadays, most passive remote sensing systems are based on satellites, designed for monitoring surface conditions of the earth and providing long-term, continuous data for the whole globe. In the current project, we used passive remote sensing data (satellite data) since they have several advantages. First, the project needs data for a number of cities in Asia and Africa, and satellites can provide all the data. Also, satellites can provide data for the required time periods since they are producing data continuously. In addition, the cost of satellite remote sensing data is less than that of airborne remote sensing. Some satellites even provide free data for all users (e.g. Landsat data).

Remote sensing systems differ in the level of detail or resolution they can capture. There are four different aspects of resolution important in remote sensing: spatial, spectral, radiometric and temporal. Spatial resolution refers to the smallest feature discernible in an image. Spectral resolution refers to the number and width of spectral bands recorded for an image. The number of values available to record the brightness levels in an image is a measure of radiometric resolution, while temporal resolution refers to the frequency of image acquisition. These four sensor characteristics need to be considered in the selection of remote sensing data best suited for a specific application (Aronoff 2005). Based on spatial resolution, satellite imageries can be categorized into three: low, medium and high spatial resolution.

2.1. Low spatial resolution satellite imageries

Low spatial resolution satellites produce coarser images (e.g. Fig. 2.1) than the other two types. In some cases, however, low-resolution satellite images have their own advantages. For example, when a LULC classification needs to be done for a large area, low spatial resolution satellite imageries can reduce the cost and time in collecting and processing since they have a relatively larger coverage. The Moderate Resolution Imaging Spectroradiometer (MODIS) and

Advanced Very High Resolution Radiometer (AVHRR) are two examples of low spatial resolution satellite sensors.

Fig. 2.1. Low spatial resolution image (500 m): MODIS image of Hawaii
Data source: http://modis.gsfc.nasa.gov
RGB Combination: True color (Red band 1; Green band 4; Blue band 3)
Date: 2014.12.20

MODIS

MODIS is a payload scientific instrument launched into earth orbit by NASA in 1999 on board the Terra (EOS AM) satellite, and in 2002 on board the Aqua (EOS PM) satellite. The MODIS instrument is the primary sensor for capturing global-coverage data on EOS AM and EOS PM satellites. It has a wide swath of 2330 km and provides coverage of the earth in 1 to 2 days. The instrument provides 36 spectral bands ranging from 0.4 µm to 14.4 µm wavelength at spatial resolutions of 250 m (2 bands), 500 m (5 bands) and 1 km (29 bands) (http://modis.gsfc.nasa.gov). They are designed to provide measurements in large-scale global dynamics including changes in the earth's cloud cover, radiation budget and processes occurring in the oceans, on land and in the lower atmosphere (Abtew & Melesse 2012).

NOAA AVHRR

The AVHRR is a broadband, four- or five-channel scanner (depending on the model), sensing in the visible, near-infrared and thermal infrared portions of the electromagnetic spectrum. The AVHRR is a radiation-detection imager that can be used for remotely determining cloud cover and surface temperature (http://noaasis.noaa.gov). The AVHRR sensors produce imagery data with a spatial resolution of 1.1 km GSD in five or six wavelength bands, depending on the satellite. The imagery is received as a continuous image covering a 2400 km-wide area. The data are supplied in two formats: 1.1 km spatial resolution local area coverage (LAC) imagery and 4 km spatial resolution global area coverage (GAC) imagery. The data is used in a

variety of time-critical and large-area applications (Aronoff 2005). Examples include weather forecasting, assessment of snow coverage and depth, monitoring of crop conditions and forest fire detection.

2.2. Medium spatial resolution satellite imageries

Medium spatial resolution satellites (multispectral: 5 m to 250 m) such as the Advanced Spaceborne Thermal Emission and Reflection Radiometer (ASTER), Advanced Land Observing Satellite (ALOS), SPOT (Satellite Pour l'Observation de la Terre, French for "earth observation") and Landsat TM/ETM+/OLI are used in the generation of quantitative LULC maps for regional scale land-change studies (Powell et al. 2007). Medium spatial resolution satellite imageries (e.g. Fig. 2.2) enable applications in various fields such as agriculture, forestry, geology, archaeology, and urban and regional land-use planning. Using ASTER imageries, Pareta & Pareta (2011) were able to study forest carbon management. In Sabah, Malaysian Borneo, Morel et al. (2011) were able to estimate the above-ground biomass in forest and oil palm plantation using ALOS PALSAR data. And in Madrid, Hewitt & Escobar (2011) were able to examine the territorial dynamics and detect the changes in fast-growing regions with Landsat imageries. Many researchers in the field of remote sensing and geospatial sciences select images in this category because they have acceptable resolution for common requirements and relatively acceptable cost (some satellites provide images for free).

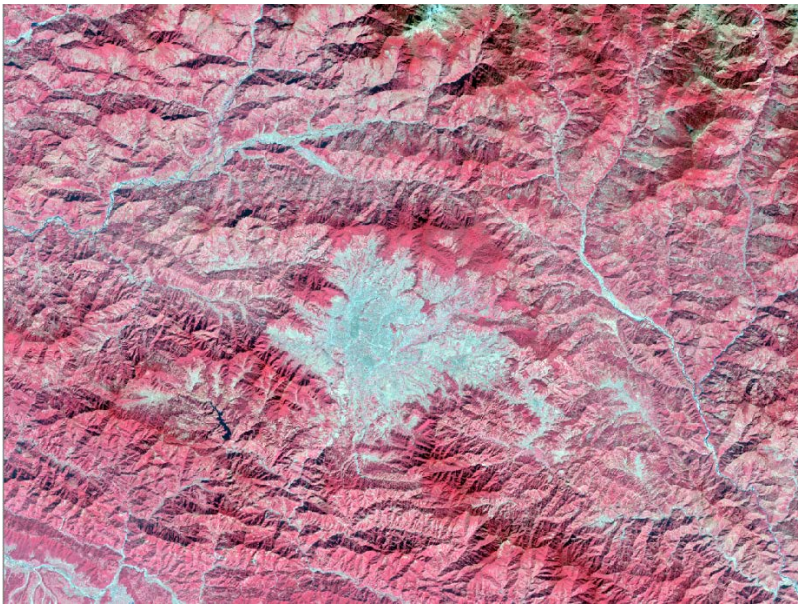

Fig. 2.2. Medium spatial resolution image (30 m): Landsat-8 image of Kathmandu
Data source: http://earthexplorer.usgs.gov
RGB Combination: Color Infrared (Red band 5; Green band 4; Blue band 3)
Date: 2013.11.18

Landsat

The Earth Resources Technology Satellite (ERTS-1), which is known as Landsat-1, was the first satellite designed to provide systematic global coverage of earth resources (Aronoff 2005). Later, the Landsat program launched a series of satellites named from Landsat-2 to Landsat-8.

The Landsat sensors collect data with a regular 16-day revisit and therefore a large amount of archived data may be available (Dalsted et al. 2003). Of the suite of medium spatial resolution satellites, Landsat is the most widely used for earth observation applications. A survey by the American Society for Photogrammetry and Remote Sensing found that the majority of respondents (71%) use Landsat as their primary source of medium spatial resolution satellite data (Powell et al. 2007). The popularity of Landsat data can be attributed to several key characteristics of the Landsat program, including a systematic data acquisition plan and archive that ensures global coverage and data availability. Further, low imagery costs and free data distribution facilitate widespread use. The keys to Landsat's popularity also include its data characteristics, namely its large footprint, and a spatial resolution fine enough to characterize typical land cover dynamics related to land management.

ASTER

ASTER is a Japanese sensor that is one of five remote sensory devices on board the Terra satellite launched into earth orbit by NASA in 1999 (http://asterweb.jpl.nasa.gov). The instrument has been collecting superficial data since February 2000. ASTER provides images of the planet earth in 14 different bands of the electromagnetic spectrum, ranging from visible to thermal infrared light. The spatial resolution of images ranges from 15 to 90 m. ASTER consists of three instruments: the visible and near-infrared (VNIR), the shortwave infrared (SWIR) and the thermal infrared (TIR). VNIR produces imageries in four bands with a spatial resolution of 15 m, SWIR offers 30 m spatial resolution imageries with six bands, and TIR has five bands with a spatial resolution of 90 m. ASTER data are used to measure snow and ice distribution, vegetation types, rock and soil properties, surface temperature and cloud properties (Aronoff 2005).

ALOS

ALOS, which has a Japanese name, "DAICHI" was launched by the Japan Aerospace Exploration Agency (JAXA) in January 2006. The dimensions of ALOS are 3.5 m wide × 4.5 m long × 6.5 m high, and its gross weight is approximately 4 tons; one of the largest among land observing satellites. ALOS has three remote sensing instruments, namely the PRISM, AVNIR-2 and PALSAR (Remote Sensing Technology Center of Japan). The Panchromatic Remote-sensing Instrument for Stereo Mapping (PRISM) is a panchromatic radiometer with high resolution in order to obtain terrain data including elevation. The Advanced Visible and Near Infrared Radiometer type 2 (AVNIR-2) is a visible and near-infrared radiometer for observing land and coastal zones and provides better spatial resolution. Lastly, the Phased Array type L-band Synthetic Aperture Radar (PALSAR) is a phased array-type L-band synthetic aperture radar, an active microwave sensor for cloud-free and day and night land observation. The major missions of ALOS include cartography, regional observation, disaster monitoring and resource surveying (JAXA 2008).

SPOT

SPOT is a commercial earth observation satellite system operating from space, run by Spot Image, based in Toulouse, France. It was designed to improve the knowledge and management of the earth by exploring the earth's resources, detecting and forecasting phenomena involving climatology and oceanography, and monitoring human activities and natural phenomena (http://www.cnes.fr). The SPOT system has already launched seven satellites (named SPOT 1 to

SPOT 7). With a 60 km wide swath, the SPOT satellites provide a coverage of the earth within 26 days. SPOT 1, 2, 3 and 4 capture both panchromatic and multispectral imagery with a spatial resolution of 10 m and 20 m respectively. SPOT 5, which was launched in 2002, has a spatial resolution of 2.5 to 5 m in panchromatic mode and 10 m in multispectral mode. Further, SPOT 6 and SPOT 7, launched in 2012 and 2014, have a higher spatial resolution of 1.5 m in panchromatic mode and 6 m in multispectral mode.

2.3. High spatial resolution satellite imageries

High spatial resolution satellite sensors require higher capacity in computer storage and higher data processing speed. So they appeared later than low and medium spatial resolution satellite sensors. High spatial resolution satellites are operated as commercial ventures. Image acquisition programs are tailored to produce commercial products of selected locations to meet the needs of government and private-sector clients (Aronoff 2005). High spatial resolution satellite imageries (e.g. Fig. 2.3) are the basis for the generation of qualitative land-use maps (i.e. land-use zoning maps) and the delineation of transportation networks (Lwin et al. 2012). High spatial resolution satellites have the highest-quality images, but also have the most expensive ones among the three types of satellites. QuickBird and IKONOS are examples of high spatial resolution satellite sensors.

Fig. 2.3. High spatial resolution image (0.61 m): Pansharpened QuickBird image of AZADI Tower in Tehran
Data source: http://www.satimagingcorp.com
RGB Combination: Natural Color (Red band 3; Green band 2; Blue band 1)
Date: 2009.6.26

IKONOS

IKONOS is a commercial earth observation satellite, and was the first to collect publicly available high spatial resolution imagery at 1 and 4 m spatial resolution. It offers multispectral and panchromatic imageries. The system is point based, allowing viewing at angles of up to ±45° in the across-track or along-track directions (Aronoff 2005). This provides more frequent imaging of a given area. The IKONOS launch was called "one of the most significant developments in the history of the space age" (Bergquist 2011).

QuickBird

QuickBird is a high spatial resolution commercial earth observation satellite owned by DigitalGlobe. It was launched in 2001 as the first satellite in a constellation of three scheduled to be in orbit by 2008. QuickBird the uses Ball Aerospace's Global Imaging System 2000, known as BGIS 2000. The satellite collects panchromatic (black and white) imagery at 61 cm resolution and multispectral imagery at 1.63 m to 2.44 m resolution, as orbit altitude is lowered during the end of mission life (https://www.digitalglobe.com). At this resolution, buildings and other infrastructure are clearly visible. However, this resolution is insufficient for working with smaller objects such as a license plate on a car! The imagery can be imported into remote sensing image processing software, as well as into GIS packages for analysis. The imagery can also be used as a backdrop for mapping applications, such as Google Earth and Google Maps.

In general, higher spatial resolution images supply more information. However, it should be mentioned that high spatial resolution is not always the best choice. Cost and necessity also need to be considered. If the goal of remote sensing is to identify large abnormal areas, then the pixel size can be increased with the size of the abnormality. If the users intend to use remote sensing data for direct ground scouting, then sufficient resolution to identify land features may be needed (Dalsted et al. 2003).

Table 2.1 summarizes the characteristics of satellite sensors widely used for earth resource remote sensing. In the current project, Landsat satellite imageries are selected based on the following considerations: resolution requirements, turnaround and revisit period, spectral bands measured by the sensor and data processing requirements. As mentioned earlier, the popularity of Landsat data can be attributed to several key characteristics of the Landsat program, including a systematic data acquisition plan and archive that ensures global coverage and data availability. The current project requires a data set for over 10 major cities in Asia and Africa. Landsat images are available since they have a worldwide coverage. Further, this project is aimed at detecting the LULC changes in each city during the 2000 and 2014 epochs, for which Landsat imageries are available. Landsat-5, -7 and -8 supply imageries every 16-day revisit period, so it is relatively easier to find good imageries for such a purpose.

Table. 2.1. Characteristics of satellite sensors widely used for earth resource remote sensing.

Platform	Sensor	Band number	Channel	Wavelength (μm)	Spatial resolution (m)	Revisit or cycle period	Swath width
NASA Terra and Aqua satellites[1]	MODIS[1]	1 2 3 4 5–7 8–10 11–12 13–14 15–19 20–25 26 27–36	Red NIR Blue Green SWIR Blue Green Red NIR TIR SWIR TIR	620–670 841–876 459–479 545–565 (see footnote) 1.36–1.39 	250 250 500 500 500 1000 1000 1000 1000 1000 1000 1000	1–2 days	2330 km
NOAA 11,12, 14,15, 16,17[2]	AVHRR	1 2 3A 3B 4 5	Green, Red NIR SWIR SWIR TIR TIR	0.58–0.68 0.73–1.00 1.58–1.64 3.55–3.93 10.30–11.30 11.50–12.50	1100	12 hours	2400 km
Landsat-5[3]	TM	1 2 3 4 5 6 7	Blue Green Red NIR SWIR 1 TIR SWIR 2	0.45–0.52 0.52–0.60 0.63–0.69 0.76–0.90 1.55–1.75 10.4–12.5 2.08–2.35	30 30 30 30 30 120 30	16 days	185 km
Landsat-7[4]	ETM+	1 2 3 4 5 6 7 8	Blue Green Red NIR SWIR 1 TIR SWIR 2 Pan	0.45–0.52 0.52–0.60 0.63–0.69 0.77–0.90 1.55–1.75 10.4–12.5 2.09–2.35 0.52–0.90	30 30 30 30 30 60 30 15	16 days	185 km
Landsat-8[5]	OLI/TIRS	1	Coastal	0.43–0.45	30	16 days	185 km

[1] http://modis.gsfc.nasa.gov/about/specifications.php

[2] http://noaasis.noaa.gov/NOAASIS/ml/avhrr.html

[3] http://landsat.usgs.gov/about_landsat5.php

[4] http://landsat.usgs.gov/about_landsat7.php

		2 3 4 5 6 7 8 9 10 11	Blue Green Red NIR SWIR 1 SWIR 2 Pan Cirrus TIRS 1 TIRS 2	0.45–0.51 0.53–0.59 0.64–0.67 0.85–0.88 1.57–1.65 2.11–2.29 0.50–0.68 1.36–1.38 10.60–11.19 11.50–12.51	30 30 30 30 30 30 15 30 100 100		
Terra[6]	ASTER[6]	1 2 3 4–9 10–14	Green Red NIR SWIR TIR	0.52–0.60 0.63–0.69 0.78–0.86 (see footnote)	15 15 15 30 90	By request	60 km
SPOT 1, 2 & 3[7]	HRV	P 1 2 3	Pan Green Red NIR	0.51–0.73 0.50–0.59 0.61–0.68 0.78–0.89	10 20 20 20	26 days	60 km
SPOT 4[7]	HRVIR	M 1 2 3 4	Mono Green Red NIR SWIR	0.61–0.68 0.50–0.59 0.61–0.68 0.78–0.89 1.58–1.75	10 20 20 20 20	26 days	60 km
SPOT 5[7]	HRG	P 1 2 3 4	Pan Green Red NIR SWIR	0.48–0.71 0.50–0.59 0.61–0.68 0.78–0.89 1.58–1.75	2.5 or 5 10 10 10 20	26 days	60 km
SPOT 6 &7[8]	NAOMI	P 1 2 3 4	Pan Blue Green Red NIR	0.45–0.75 0.45–0.52 0.53–0.59 0.62–0.69 0.76–0.89	1.5 6 6 6 6	26 days	60 km

[5] http://landsat.usgs.gov/landsat8.php

[6] http://www.satimagingcorp.com/satellite-sensors/other-satellite-sensors/aster/; http://www.science.aster.ersdac.jspacesystems.or.jp/jp/documnts/users_guide/part2/01.html

[7] http://www.blackbridge.com/geomatics/upload/airbus/SPOT1-5%20Resolutions%20and%20Spectral%20Modes.pdf

[8] http://www.satimagingcorp.com/satellite-sensors/spot-6/; http://www.satimagingcorp.com/satellite-sensors/spot-7/

ALOS[9]	PRISM AVNIR-2 PALSAR	P 1 2 3 4	Pan Blue Green Red NIR	0.52–0.77 0.42–0.50 0.52–0.60 0.61–0.69 0.76–0.89	2.5 10 10 10 10 10 and 100	46 days	70 km
IKONOS[10]	Panchro- matic Multi- spectral	P 1 2 3 4	Pan Blue Green Red NIR	0.45–0.90 0.45–0.52 0.51–0.60 0.63–0.70 0.76–0.85	1 4 4 4 4	1.5–3 days	11 km
QuickBird[11]	Panchro- matic Multi- spectral	P 1 2 3 4	Pan Blue Green Red NIR	0.45–0.90 0.45–0.52 0.52–0.60 0.63–0.69 0.76–0.90	0.61 2.44 2.44 2.44 2.44	1–3.5 days	16.5 km

[9] http://www.eorc.jaxa.jp/ALOS/en/about/about_index.htm

[10] http://www.satimagingcorp.com/satellite-sensors/ikonos/

[11] http://glcf.umd.edu/library/guide/QuickBird_Product_Guide.pdf

3. Overview of classification methods, study areas and data processing

3.1. Overview of classification methods

Image classification refers to the task of extracting information from a multiband raster image. Depending on the interaction between the analyst and the computer during classification, there are two types of classification: supervised and unsupervised. Supervised classification requires *a priori* knowledge of the data and study area. It is a widely used technique for extracting quantitative information from remotely sensed image data, where samples or training data are used in the classification process. On the other hand, unsupervised classification does not require *a priori* knowledge. It is done mainly by using some clustering algorithms to classify an image (Richards 1993). Aside from these two groups of classification methods (supervised and unsupervised), classification methods can also be grouped into two, i.e. pixel-based and object-based. Machine learning algorithms have also emerged, including random forests and support vector machines. These are described below.

Pixel-based classification and object-based classification

The development and advancement of geographic object-based image analysis (GEOBIA) (Hay & Castilla 2008; Blaschke et al. 2014) techniques provides an alternative to the traditional pixel-based classification approach. In a pixel-based classification, an entire digital image is processed pixel by pixel using spectral information. On the other hand, in a GEOBIA technique, pixels are group into objects based on spectral, shape, texture and contextual information through image segmentation (Platt & Rapoza 2008; Blaschke 2010). Image segmentation is a process of partitioning an image into isolated objects so that each object shares a homogeneous spectral similarity (Blaschke et al. 2004). However, amidst the advancement of GEOBIA techniques, pixel-based classification still remains the basis for thousands of remote sensing applications (Blaschke 2010). The limited access of researchers to software packages that support GEOBIA might be one of the reasons behind this. In addition, pixel-based classification techniques can also provide accurate and satisfactory results.

Random Forests classification

"Random Forests" (RF) is a machine learning method that uses a collection of tree-structured classifiers for classification (Breiman 2001). It is an ensemble classification method and a learning algorithm that assembles a set of classifiers instead of one classifier, and then classifies new data points by taking a vote of their predictions (Breiman 2001; Liaw & Wiener 2002; Akar & Gungor 2012). RF is an advanced version of bagging (Breiman 2001), in which randomness is added (Akar & Gungor 2012). The key advantages of RF algorithms are their nonparametric nature, high classification accuracy, and ability to determine variable importance (Rodriguez-Galiano et al. 2012).

Support Vector Machine classification

Support Vector Machines (SVMs) are based on statistical learning theory (Vapnik 1995). The primary objective of SVMs is to generate a hyperplane that represents the optimal separation of linearly separable classes in decision boundary space. Most SVM applications involve the separation of only two classes by a decision boundary termed the "optimal separating hyperplane" (OSH) (Brian et al. 2011). In general, SVMs select the decision boundary from an infinite

number of potential ones, leaving the greatest margin between the closest data points to the hyperplane, which are referred to as “support vectors” (Griffiths et al. 2010).

For the purpose of this project, we used the supervised classification method, employing the maximum likelihood algorithm. We used our knowledge of the study areas and skills in the interpretation of remote sensing satellite imageries and development of training areas. The maximum likelihood algorithm is one of the most widely used algorithms in satellite image classification. It is based on the Bayes’ theorem (Richards 1993).

3.2. Study areas

Over the past few decades, urbanization in various countries, including Asian and African countries, has been rapid. The primary objective of this project is to establish a database of LULC maps derived from remote sensing satellite imageries during this time period for various major Asian and African cities. It also aims to detect the changes in the landscape of these cities and examine how the spatial structure of each city has changed over the years.

In this project, the study areas include 11 major Asian cities (Bangkok, Thailand; Beijing, China; Dhaka, Bangladesh; Hanoi, Vietnam; Jakarta, Indonesia; Kathmandu, Nepal; Kuala Lumpur, Malaysia; Manila, Philippines; Seoul, South Korea; Taipei, Taiwan; and Tehran, Iran) and two major African cities (Bamako, Mali; Nairobi, Kenya). The spatiotemporal dimensions of LULC changes in these cities during the 2000 and 2014 epochs were examined. For the purpose of an objective comparison, we used a standardized unit of analysis, i.e. a 100 km × 100 km study area for each city.

3.3. Data processing

For the purpose of this project, eight LULC classes were considered: urban dense, urban sparse, forest, cropland, grassland, bareland, water and other land. The other land class includes clouds, shadow and snow. The same LULC classes have been used in previous studies (e.g. Lwin & Murayama 2013).

We first searched the best remote sensing satellite imageries (Landsat data) for the two epochs (2000 and 2014), i.e. cloud-free or with minimal cloud cover. The selected imageries, which are all Level 1T products, were downloaded from http://earthexplorer.usgs.gov. In the Level 1T product type, the imageries have been geometrically corrected. Subsequently, the study area (100 km × 100 km) in each city was clipped, processed and classified using the maximum likelihood supervised classification method explained above.

4. LULC classification results

In this chapter, the results of the LULC classifications for the 13 cities are presented. The 11 Asian cities are presented first, alphabetically, followed by the two African cities. It should be noted that the total land area of each study site is based on the classified LULC maps (100 km × 100 km) and does not necessarily correspond to the cities' respective administrative land area.

4.1. Bangkok Metropolitan Region, Thailand

Geographical and socioeconomic characteristics

The Bangkok Metropolitan Region (BMR) houses Thailand's capital city, Bangkok. BMR has a total land area of 7762 km^2, and it is managed by the Bangkok Metropolitan Administration. Geographically, Bangkok is situated at latitude 13^o 45' North and longitude 100^o 28' East, along the banks of the Chao Phraya River, which extends to the Gulf of Thailand. The other five provinces that comprise the BMR are the provinces of Samut Prakarn, Samut Sakhon, Nonthaburi, Pathu Thani and Nakhon Pathom.

While Bangkok serves as the BMR's headquarters for numerous multinational companies and the country's center for major financial institutions, it is also one of Asia's commercial and transport hubs and one of the world's most popular tourist destinations (Siemens 2011; ADB 2014). Due to the dominance and influence of BMR, it has been reported that any adverse effect on its socioeconomics will certainly have a negative influence on the socioeconomics of the whole country (World Bank 2009).

In 2000, BMR had a population of 10.2 million and a density of 1309 people/km^2, while in 2010 these figures increased to 14.6 million and 1884 people/km^2, respectively (http://www.citypopulation.de). In 2000, BMR's population represented 16.68% of the total population of Thailand, while in 2010, it accounted for 22.17%. According to ADB (2014), the increase in BMR's population from 2000 to 2010 contributed to a decrease in the quality of infrastructure and service provision in the region, as it also increased the city's poverty index because most immigrants from the rural areas had low levels of education and income, and poor housing conditions. In addition, due to the flatness of the area and its proximity to the seashore, the area annually faces the problems of floods from the water from the north and inundation due to the high tide from the sea (World Bank 2009).

LULC changes in Bangkok Metropolitan Region

Basically, the landscape of BMR is dominated by cropland, with patches of forest cover and grasslands. Figures 4.1(a) and 4.1(b) show the classified LULC maps of BMR, while Figure 4.1(c) highlights the detected urban land changes between 1999 and 2014, including the changes from urban sparse to urban dense (red), non-urban to urban dense (blue), and non-urban to urban sparse (green). Spatially, it can be observed that urban dense and urban sparse have been expanding outward of the city core and along major roads (Fig. 4.1(c)). There are also signs that some smaller cores are developing, especially in the western, northern and southeastern parts of BMR (Fig. 4.1). In 1999, the area of urban dense was 32.78 thousand ha, i.e. 3.28% of the whole landscape (Table 4.1). In 2014, it increased to 117.59 thousand ha, i.e. 11.76% of the landscape, showing a remarkable net increase of 258.72% from 1999. The increase in the land area of urban dense was due to its gains from non-urban areas, but more especially from urban sparse. On the other hand, the area of urban sparse decreased from 102.94 thousand ha (10.29%) in 1999 to 100.83 thousand ha in 2014 (10.08%) (Table 4.1), with a net decrease of 2.05% during the 1999–

2014 period. This is despite its gains from non-urban areas (Fig. 4.1(c)). The decrease of the land area of urban sparse was mainly due to its loss to urban dense, which was greater than the area it gained from the non-urban areas. This shows that while there are indications of urban sprawl in BMR, there are also signs of an infilling pattern.

The other important LULC of BMR, i.e. forest and cropland, also had substantial changes in their respective land area between 1999 and 2014. Based on the two LULC maps (Figs. 4.1(a) and 4.1(b)) and the detected changes (Table 4.1), more than a half of BMR's forest cover was converted to other uses during the 1999–2014 period. During the same period, its cropland also decreased by more than 6%. The details of the changes for the other LULC classes are summarized in Table 4.1. Overall, the data show that BMR has been experiencing remarkable landscape changes, posing many challenges in the context of landscape and urban planning for its sustainable urban development.

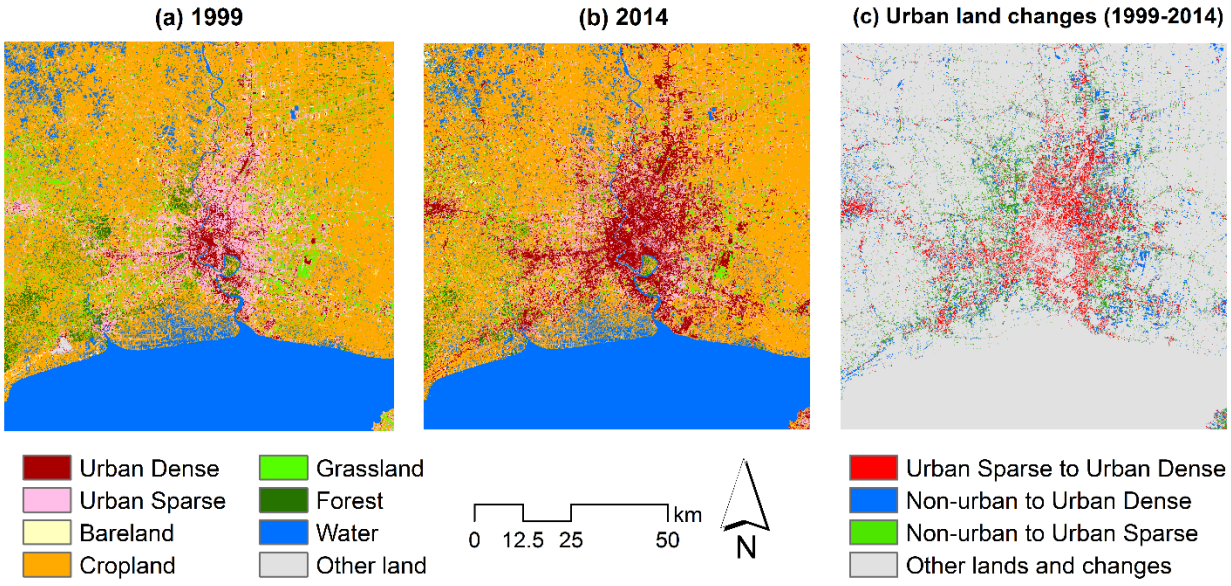

Fig. 4.1. LULC maps and spatial distribution of urban land changes in BMR.

Table 4.1. LULC changes in BMR (1999–2014).

	1999		2014		Net Changes (1999–2014)	
	ha ('000)	% of total	ha ('000)	% of total	ha ('000)	% of 1999
Urban Dense	32.78	3.28	117.59	11.76	84.81	258.72
Urban Sparse	102.94	10.29	100.83	10.08	-2.11	-2.05
Forest	35.93	3.59	15.44	1.54	-20.49	-57.04
Cropland	497.87	49.78	466.71	46.67	-31.16	-6.26
Grassland	61.69	6.17	38.34	3.83	-23.36	-37.86
Bareland	13.45	1.34	11.21	1.12	-2.24	-16.66
Water	253.66	25.36	249.92	24.99	-3.74	-1.47
Other land	1.77	0.18	0.07	0.01	-1.71	-96.17
Total	1000.10	100.00	1000.10	100.00		

4.2. Beijing Metropolitan Area, China

Geographical and socioeconomic characteristics

As the capital of China, Beijing is the second largest Chinese city by urban population and it is the nation's political, cultural and educational center. Beijing is also one of the most populous cities in the world. Its population in 2013 was 21,150,000. The city proper is the third largest in the world (http://www.globaltimes.cn). The land area of Beijing is about 16,410 km^2 (http://english.mofcom.gov.cn), which is the largest capital city in our project. In the 1980s, the metropolitan area of Beijing was about 1500 km^2 only, but soon expanded due to the Chinese economic reform.

In recent years, the population of Beijing has also been growing at breakneck speed. Between the 2000 and 2010 census periods, the number of people living in the city grew by 44% – from 13,569,194 in 2000 to 19,612,368 in 2010. The average growth rate of cities since the 1960s has been around 20% per decade (http://worldpopulationreview.com). Although Beijing is a historical city, its urbanization process has been incredible. This has been due to the Chinese economic reform and economic globalization.

LULC changes in Beijing Metropolitan Area

Figures 4.2(a) and 4.2(b) show the LULC classification results for Beijing using the maximum likelihood supervised classification method. Figure 4.2(c) highlights the detected LULC changes from non-urban to urban sparse (green), non-urban to urban dense (blue) and urban sparse to urban dense (red) between 2002 and 2014. The gray areas are other lands and changes. Table 4.2 shows the statistics of the eight LULC categories and the detected changes between 2002 and 2014 for Beijing. The category "other land" refers to cloud and shadow. More specifically, the area and percentage of each LULC class, including the detected net changes are summarized in Table 4.2.

There are some differences between Beijing and the other cities. Firstly, unlike the capital cities of other Asian or African countries, Beijing is a big city, which has been almost fully developed. Spatially, Beijing's urban area radiates from the center (the Forbidden City). Secondly, Beijing is situated in the northern tip of the roughly triangular North China Plain. Mountains to the north, northwest and west shield the city and northern China's agricultural heartland from the encroaching desert steppes. But despite this, Beijing still has a major water security problem. In addition, Beijing has a rather dry, monsoon-influenced, humid continental climate. Consequently, there have been some misclassifications in rural areas, where some cropland areas have been misclassified as bareland. Thirdly, because of the unique culture of China, people prefer to live together rather than separately. Even in small villages, the residential houses are built next to each other, and are surrounded by agricultural lands. This pattern resulted to 'urban dense'.

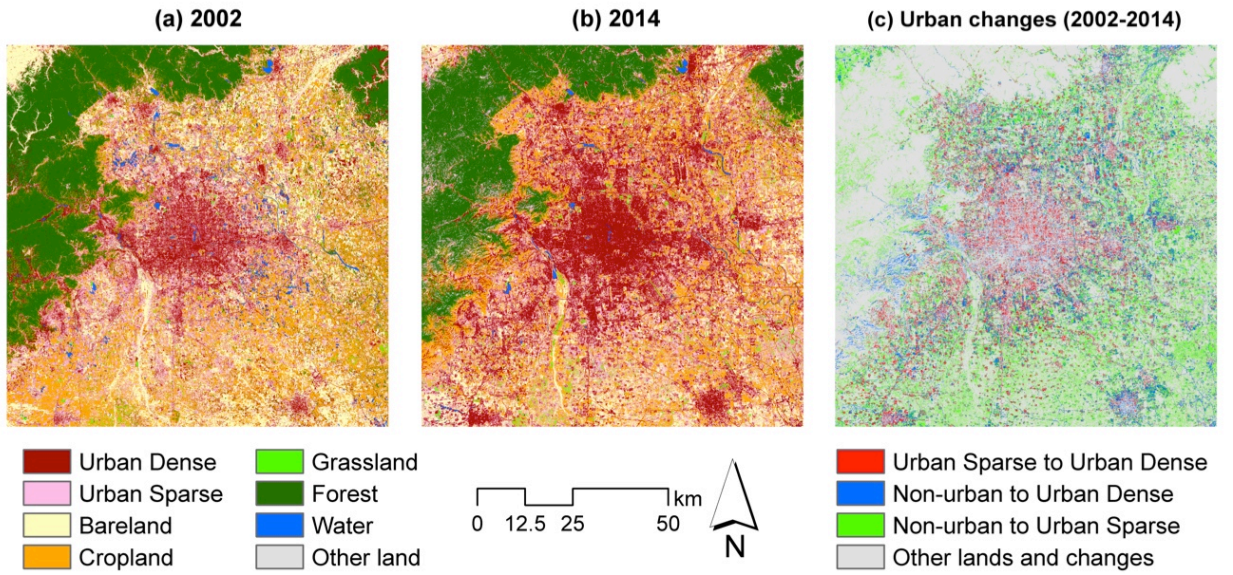

Fig. 4.2. LULC maps and spatial distribution of urban land changes in Beijing Metropolitan Area.

Table 4.2. LULC changes in Beijing Metropolitan Area (2002–2014).

	2002		2014		Net Changes (2002–2014)	
	ha ('000)	% of total	ha ('000)	% of total	ha ('000)	% of 2002
Urban Dense	149.40	14.93	241.35	24.13	91.95	61.55
Urban Sparse	176.30	17.62	253.52	25.34	77.23	43.80
Forest	206.46	20.64	168.66	16.86	-37.80	-18.31
Cropland	219.78	21.97	213.43	21.33	-6.35	-2.89
Grassland	8.73	0.87	15.28	1.53	6.55	75.03
Bareland	225.93	22.58	98.29	9.83	-127.64	-56.49
Water	13.80	1.38	4.64	0.46	-9.16	-66.36
Other Land	0.00	0.00	5.22	0.52	5.22	---
Total	1000.40	100.00	1000.40	100.00		

4.3. Dhaka Metropolitan Area, Bangladesh

Geographical and socioeconomic characteristics

Dhaka metropolitan is commonly known as the Greater Dhaka Area (GDA). Administratively, the metropolitan area is called the Dhaka Statistical Metropolitan Area (SMA), and comprises the Dhaka City Corporation (DCC), Keraniganj Demra, Narayangoni, Dhaka Contonmenet, Tongi and adjoining rural area (Chowdhury 2007). Dhaka City, the capital of Bangladesh, is located in the Dhaka metropolitan region. Geographically, Dhaka is located at latitude 23° 43′ North and longitude 90° 25′ East and is situated in the great delta region of the Ganges and Brahmaputra rivers. A large area of Dhaka is covered by a flat wetland. Its elevation ranges from 0.5 m to 12 m above sea level.

Dhaka is one of the major cities of South Asia. Being a member of the "megacity" family of the world, it is also one of the world's most densely populated cities. According to the 2001 census, the Dhaka Statistical Metropolitan Area (SMA) accommodates 10.7 million people, which is 37.45% of the total urban population of Bangladesh (http://www.bbs.gov.bd). The UN ranked Dhaka City as the 11th biggest population agglomeration in the world; it had a 3.6% annual growth rate from 2010 to 2015 (UN 2014).

The GDA is one of the major business hubs of South Asia and it is one of the fast-growing economic regions in Asia. The largest industrial sectors of Dhaka are textiles, jute, cement, ceramics, construction materials, newsprint, accessories, leather goods, electronics and appliances. Various estimates indicate that up to one quarter of Dhaka's population lives in informal settlements (shantytowns, slums or favelas). Additionally, the geographical location of Dhaka poses some social and environmental problems like flooding.

LULC changes in Dhaka Metropolitan Area

Figures 4.3(a) and 4.3(b) show the LULC classification results for Dhaka using the maximum likelihood supervised classification method. Figure 4.3(c) highlights the detected LULC changes from non-urban to urban sparse (green), non-urban to urban dense (blue), urban sparse to urban dense (red) and other lands and changes (gray) between 2000 and 2014. The urban land use is located at the center of the study area. It can be noted that the spatial urban expansion of Dhaka is greatly limited by the two rivers surrounding the city. Urban dense is spatially arranged along the riverbank. Cropland is mixed with the urban land use as the city is located on a floodplain. It is clear that urban sparse has been expanding outward of the city center, while the urban sparse at the city core has been converted to urban dense. The major river (water class) that flows through the Dhaka metropolitan area was dynamic.

In 2000, the area of urban dense was 4.39 thousand ha, covering 0.44% of the whole landscape (Table 4.3). In 2014, it increased to 10.88 thousand ha, i.e. 1.09% of the landscape. From 2000 to 2014, urban dense had a net increase of 6.49 thousand ha. The area of urban sparse in 2000 was 16.33 thousand ha only (1.63%), but in 2014, it increased to 61.78 thousand ha (6.18%), with a net increase of 278.32%. Among the eight LULC classes of Dhaka, cropland is the most dominant. It accounted for 43.64% (436.620 thousand ha) in 2000 and 53.59% (536.16 thousand ha) in 2014. The second major LULC type is forest, covering 403.83 thousand ha (40.37%) in 2000 and 298.39 thousand ha (29.83%) in 2014. The net decrease in the area of forest from 2000 to 2014 was substantial (-26.11% or 105.44 thousand ha). On the other hand, the area of cropland increased by 22.80% (99.54 thousand ha). The details of the changes for the other LULC classes are summarized in Table 4.3. Overall, the LULC changes in the Dhaka metropolitan area show a sizable urban expansion, with a declining forest cover.

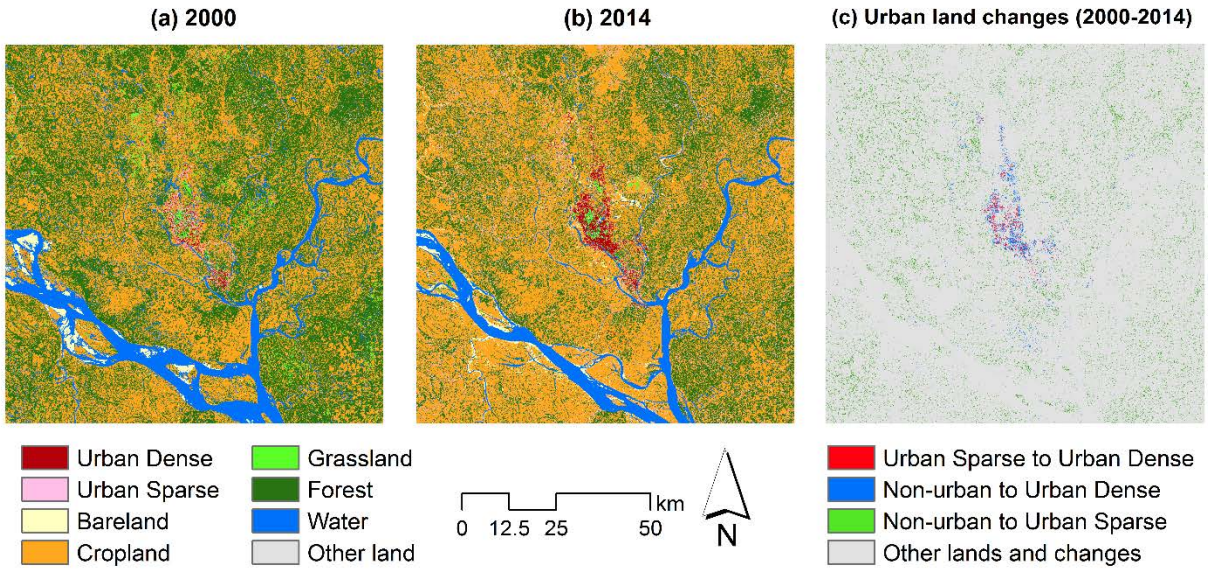

Fig. 4.3. LULC maps and spatial distribution of urban land changes in Dhaka Metropolitan Area.

Table 4.3. LULC changes in Dhaka Metropolitan Area (2000–2014).

	2000		2014		Net Changes (2000–2014)	
	ha ('000)	% of total	ha ('000)	% of total	ha ('000)	% of 2000
Urban Dense	4.39	0.44	10.88	1.09	6.49	147.75
Urban Sparse	16.33	1.63	61.78	6.18	45.45	278.32
Forest	403.83	40.37	298.39	29.83	-105.44	-26.11
Cropland	436.62	43.64	536.16	53.59	99.54	22.80
Grassland	18.31	1.83	5.80	0.58	-12.51	-68.32
Bareland	11.60	1.16	18.68	1.87	7.09	61.12
Water	109.32	10.93	68.71	6.87	-40.61	-37.15
Other land	0.00	0.00	0.00	0.00	0.00	---
Total	1000.40	100.00	1000.40	100.00		

4.4. Hanoi Metropolitan Area, Vietnam

Geographical and socioeconomic characteristics

Hanoi is the capital of Vietnam and the country's second largest city. In 2009, the population of the urban districts of Hanoi was 2.6 million (http://www.gso.gov.vn), while the population of the metropolitan area was 6.5 million (http://balita.ph). Hanoi is located in the northern region of Vietnam, situated in Vietnam's Red River delta, nearly 90 km away from the coastal area. Hanoi is 1760 km north of Ho Chi Minh City and 120 km west of Haiphong City. The landscape of Hanoi expands from the delta to the midland and mountainous regions. In general, the terrain becomes gradually lower from north to south and from west to east, with an average height ranging from 5 to 20 m above sea level. The hilly and mountainous regions are located in the northern and western part of the city.

In recent years, the sharp growth of local population, together with the unequal living standards between rural and urban areas, has created many challenges. Since Hanoi expanded its administrative boundary in 2008, merging Hanoi and Ha Tay province, the capital city's population has reached 7.1 million. In the last four years, Hanoi's population has been increasing at a rate of 0.43 million people per year (http://tuoitrenews.vn). On the average, the population has been growing at a rate of 50 thousand per year due to immigration, with working age people in the majority. In order to respond to this rapid population growth, the expansion of Hanoi's administrative boundary was an important process.

LULC changes in Hanoi Metropolitan Area

Figures 4.4(a) and 4.4(b) show the LULC classification results for Hanoi using the maximum likelihood supervised classification method. Figure 4.4(c) highlights the detected LULC changes from non-urban to urban sparse (green), non-urban to urban dense (blue) and urban sparse to urban dense (red) between 2001 and 2014. The gray areas are other lands and changes. Table 4.4 shows the statistics of LULC changes between 2001 and 2014 in Hanoi. The category "other land" refers to cloud and shadow. More specifically, the area and percentage of each LULC class, including the detected net changes are summarized in Table 4.4.

Compared with other capital cities, Hanoi is small. As a city located in a tropical region, Hanoi also has a typical tropical city characteristic: the land use and land cover are influenced by the season. There is a big difference in the LULC classification results for satellite imageries captured in rainy season and dry season. As the capital city of a developing country, Hanoi also underwent huge changes during the economic globalization. From 2001 to 2014, the area of urban dense increased by 175%, while the area of urban sparse increased by 11%.

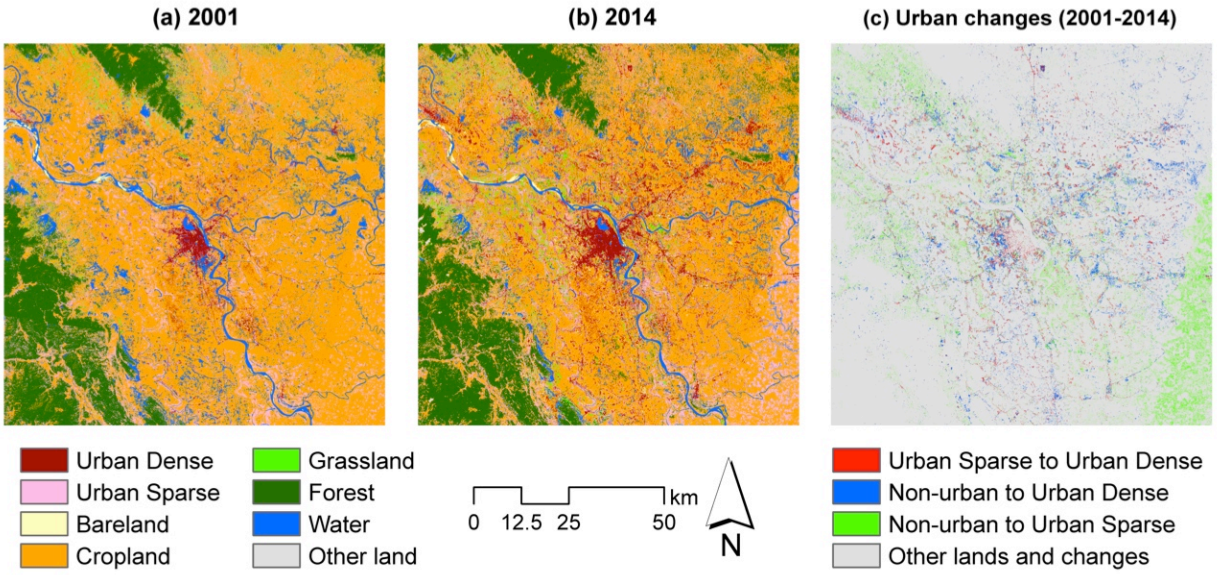

Fig. 4.4. LULC maps and spatial distribution of urban land changes in Hanoi Metropolitan Area.

Table 4.4. LULC changes in Hanoi Metropolitan Area (2001–2014).

	2001		2014		Net Changes (2001–2014)	
	ha ('000)	% of total	ha ('000)	% of total	ha ('000)	% of 2001
Urban Dense	26.83	2.68	73.79	7.37	46.96	175.02
Urban Sparse	125.17	12.51	139.81	13.97	14.64	11.70
Forest	132.57	13.25	144.47	14.44	11.90	8.98
Cropland	623.39	62.30	545.53	54.52	-77.87	-12.49
Grassland	11.28	1.13	21.29	2.13	10.01	88.78
Bareland	7.49	0.75	20.12	2.01	12.63	168.69
Water	73.91	7.39	54.90	5.49	-19.00	-25.71
Other Land	0.05	0.00	0.77	0.08	0.72	1516.79
Total	1000.68	100.00	1000.68	100.00		

4.5. Jakarta Metropolitan Area, Indonesia

Geographical and socioeconomic characteristics of Jakarta

The Jakarta metropolitan area includes the cities of Jakarta, Bogor, Depok, Tangerang and Bekasi. It is commonly identified as "Jabodetabek," and the name is derived from the first two letters of each city. The capital city of the Republic of Indonesia, Jakarta, is located in the Jabodetabek region. Geographically, Jakarta City is located at latitude 6° 08′ South and longitude 106°45′ East and it is situated on the northwest coast of the Java Island. The landscape of Jakarta is characterized by a low, flat basin, averaging 7 m above sea level. The southern part of the city is comparatively hilly, while some flat areas in the northern part are below sea level. The total land area of the Jakarta metropolitan area is about 7700 km^2, while Jakarta City has an area of about 660 km^2.

Jakarta is one of the most popular urban agglomerations in the world. The population of Jakarta City was 9.12 million in 2013 (https://www.cia.gov) and the metropolitan area of Jakarta has a population of 27 million, with an annual growth rate of 3.2 % (http://www.citypopulation.de). The UN ranked Jakarta City as the 28th largest population agglomeration in the world (UN 2014). Jakarta is also listed as a global city in the 2008 Globalization and World Cities Study Group and Network (GaWC) research (http://www.lboro.ac.uk).

The Jakarta metropolitan area is the main economic and administrative center of Indonesia. Financial services, trade and manufacturing are the main economic activities in the city. Major industries in Jakarta include electronics, automotive, chemicals, mechanical engineering and biomedical sciences manufacturing. However, the Jakarta metropolitan area has also been facing a wide range of urban problems since the last few decades, including flooding and traffic congestion.

LULC changes in Jakarta Metropolitan Area

Figures 4.5(a) and 4.5(b) show the LULC classification results for Jakarta using the maximum likelihood supervised classification method. Figure 4.5(c) highlights the detected LULC changes from non-urban to urban sparse (green), non-urban to urban dense (blue), urban sparse to urban dense (red) and other lands and changes (gray) between 2001 and 2014. The urban land use is mostly located in the northern part of city, while the southern part is covered by forest. Furthermore, it can be observed that urban dense is highly agglomerated around the port of Jakarta City, located close to the city center. It seems that the location of Jakarta port is an important factor for the development of the urban area in the northern part of the city. In addition, the international airport, many industries and administrative centers are concentrated in the northern part of the city. The urban area is expanding towards the south, following a triangular spatial pattern.

The area of urban dense was 37.89 thousand ha in 2001, covering 3.79% of the whole landscape (Table 4.5). In 2014, it increased to 81.63 thousand ha, i.e. 8.16% of the landscape, showing a net increase of 43.74 thousand ha from 2001. The area of urban sparse in 2001 was 51.78 thousand ha (5.18%), but in 2014, it increased to 80.38 thousand ha (8.03%). Furthermore, the area of cropland was 313.71 thousand ha (31.36%) in 2001 and 294.80 thousand ha (29.47%) in 2014. The area of forest was 130.91 thousand ha (13.09%) in 2001 and 118.28 thousand ha (11.82%) in 2014. The net decrease in the area of grassland from 2001 to 2014 was substantial (-41.75% or 38.75 thousand ha). The details of the changes for the other LULC classes are summarized in Table 4.5. Overall, the LULC changes in Jakarta metropolitan area from 2001 to

2014 show that urban expansion has been great. By contrast, the area of all the other LULC classes, except for bareland, has decreased.

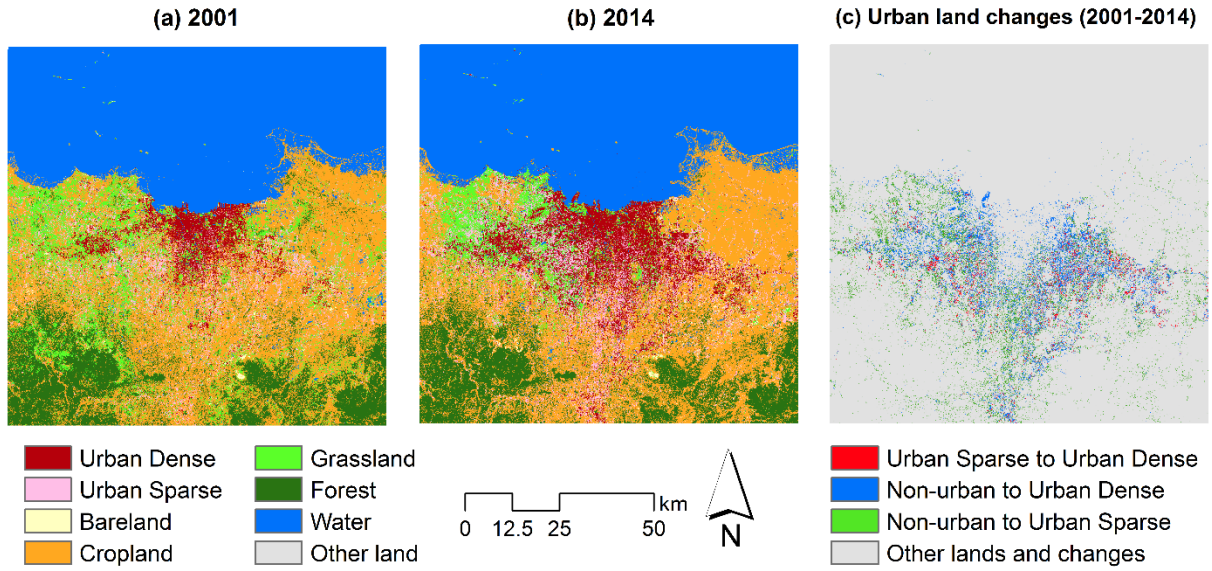

Fig. 4.5. LULC maps and spatial distribution of urban land changes in Jakarta Metropolitan Area.

Table 4.5. LULC changes in Jakarta Metropolitan Area (2001–2014).

	2001		2014		Net Changes (2001-2014)	
	ha ('000)	% of total	ha ('000)	% of total	ha ('000)	% of 2001
Urban Dense	37.89	3.79	81.63	8.16	43.74	115.44
Urban Sparse	51.78	5.18	80.38	8.03	28.60	55.24
Forest	130.91	13.09	118.28	11.82	-12.62	-9.64
Cropland	313.71	31.36	294.80	29.47	-18.91	-6.03
Grassland	92.83	9.28	54.08	5.41	-38.75	-41.75
Bareland	7.20	0.72	8.85	0.88	1.65	22.98
Water	366.07	36.59	362.37	36.22	-3.71	-1.01
Other land	0.00	0.00	0.00	0.00	0.00	---
Total	1000.39	100.00	1000.39	100.00		

4.6. Kathmandu Metropolitan Area, Nepal

Geographical and socioeconomic characteristics

Kathmandu, the political and culture capital of Nepal, is the largest municipality in the country. It is the only city in Nepal with administrative status 'metropolitan city'. The city is located at the urban core of the Kathmandu Valley in the Himalayas. Kathmandu Valley also includes two sister cities, namely Patan or Lalitpur, 5 km to the southeast, and Bhaktapur, 14 km to the east (http://www.kathmandu.gov.np). The city stands at an elevation of approximately 1400 m in the bowl-shaped valley of central Nepal. It is surrounded by four major mountains: Shivapuri, Phulchoki, Nagarjun and Chandragiri.

Kathmandu has the highest population density in the country, and is home to about a twelfth of Nepal's population. According to the census data, Kathmandu's population increased from 671,846 to 1,003,285 people from 2001 and 2011. The metropolitan area is about 49.45 km² and has a population density of 20,289 per km² (http://www.citypopulation.de).

LULC changes in Kathmandu Metropolitan Area

Figures 4.6(a) and 4.6(b) show the LULC classification results for Kathmandu using the maximum likelihood supervised classification method. Figure 4.6(c) highlights the detected LULC changes from non-urban to urban sparse (green), non-urban to urban dense (blue) and urban sparse to urban dense (red) between 2001 and 2013. The gray areas are other lands and changes.

Table 4.6 shows the statistics of LULC changes between 2001 and 2013 in Kathmandu. The category "other land" refers to snow, cloud and shadow. More specifically, the area and percentage of each LULC class, including the detected net changes are summarized in Table 4.6. Figure 4.6 shows that Kathmandu's urban area is relatively small. The urban expansion in the whole landscape from 2001 to 2013 only happened in a small part. The reason is that Kathmandu City is relatively small compared to the whole 100 km × 100 km study area. Had the area coverage of the LULC mapping been reduced, the urban expansion in Kathmandu would have been much clearer. Forest is the most dominant category since the area is located in a mountainous region covered by trees. The northeastern part of the landscape shows a large area classified as "other land." Most of this area is covered with snow.

Table 4.6 shows that the area of urban dense and urban sparse increased from 2001 to 2013. In 2001, the area of urban dense was 6.75 thousand ha, accounting for 0.67% of the whole area. In 2013, it increased to 11.67 thousand ha with a net increase of 72.91% from 2001. During the same period, the area of urban sparse also increased by 76.14%. These results show that urban expansion in Kathmandu has been substantial. On the other hand, the area of cropland decreased from 17.21% to 11.87% due to its loss to urban area. Grassland increased from 1.24% to 2.94%, while forest increased from 44.85% to 50.66%. These changes might have been influenced by the seasonal differences between the two imageries used. The 2001 image was acquired at the end of December, while the 2013 image was acquired at the beginning of November. Further, it can be observed that the category "other land" decreased from 13.03% to 5.70%. This shows that some areas covered with snow, cloud or shadow in the 2001 image were no longer covered in the 2013 image. This is also one of the possible sources of the detected LULC changes for the bareland class.

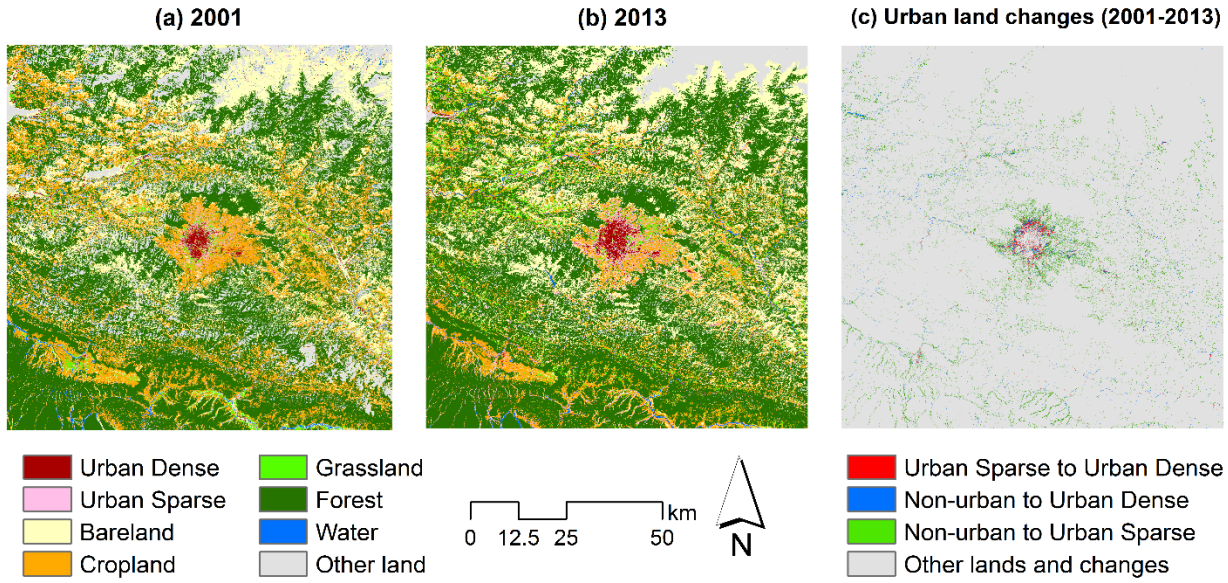

Fig. 4.6. LULC maps and spatial distribution of urban land changes in Kathmandu Metropolitan Area.

Table 4.6. LULC changes in Kathmandu Metropolitan Area (2001–2013).

	2001		2013		Net Changes (2001-2013)	
	ha ('000)	% of total	ha ('000)	% of total	ha ('000)	% of 2001
Urban Dense	6.75	0.67	11.67	1.17	4.92	72.91
Urban Sparse	21.60	2.16	38.05	3.80	16.49	76.14
Forest	448.84	44.85	506.90	50.66	58.06	12.94
Cropland	172.23	17.21	118.82	11.87	-53.41	-31.01
Grassland	12.42	1.24	29.44	2.94	17.02	137.10
Bareland	197.53	19.74	231.18	23.10	33.65	17.04
Water	10.96	1.10	7.62	0.76	-3.34	-30.50
Other land	130.37	13.03	57.02	5.70	-73.35	-56.26
Total	1000.70	100.00	1000.70	100.00		

4.7. Kuala Lumpur Metropolitan Area, Malaysia

Geographical and socioeconomic characteristics

Kuala Lumpur is the federal capital of Malaysia and the most populous city in the country. The urban area of Kuala Lumpur is more than 240 km^2 and it has an estimated population of 1.8 million (http://archive.today/toTM). Kuala Lumpur is located in the Klang Valley, bordered by the Titiwangsa Mountains in the east (http://www.visitkualalumpur.com). As one of the most important cities in Asia, it enjoys a booming economy and shows the vitality of an expanding city over the past two decades in response to globalization (http://archive.unu.edu).

Based on the Department of Statistics, Kuala Lumpur has a population of 1.67 million people, i.e. in an area of just 243 km^2 (http://www.dbkl.gov.my). This gives the city proper a very high population density of 6,890 km^2. The Greater Kuala Lumpur, or the Klang Valley, is a large urban agglomeration with an estimated population of 7 million in 2014 and a population density that is nearly equal to that of the city proper (http://worldpopulationreview.com). In the context of urbanization, Kuala Lumpur has been growing over the past three decades amidst economic globalization.

LULC changes in Kuala Lumpur Metropolitan Area

Figures 4.7(a) and 4.7(b) show the LULC classification results for Kuala Lumpur using the maximum likelihood supervised classification method. Figure 4.7(c) highlights the detected LULC changes from non-urban to urban sparse (green), non-urban to urban dense (blue) and urban sparse to urban dense (red) between 2001 and 2014. The gray areas are other lands and changes. Table 4.7 shows the statistics of LULC changes between 2001 and 2014 in Kuala Lumpur. The category “other land” refers to cloud and shadow. More specifically, the area and percentage of each LULC class, including the detected net changes are summarized in Table 4.7.

Kuala Lumpur is located in a place surrounded by mountains, and because of the limitation of land area, urban areas are concentrated in the low-lying regions. From 2001 to 2014, the area of urban dense increased by almost 60%, while area of urban sparse increased by 76% (Table 4.7). The results also show a net decrease of 36% for cropland and 21% for forest from 2001 to 2014 due to urbanization. Most of the changed areas are located in the western side of the mountain. It can be observed that for the classification in 2014, the northeastern side of Kuala Lumpur was filled with clouds and shadow, affecting the classification and change detection results.

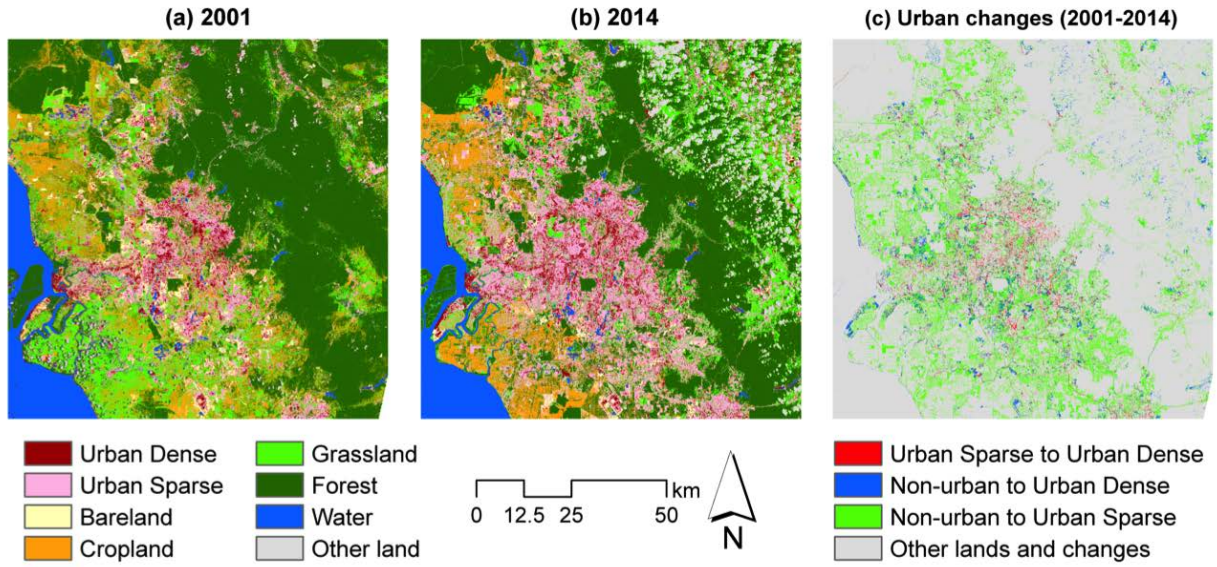

Fig. 4.7. LULC maps and spatial distribution of urban land changes in Kuala Lumpur Metropolitan Area.

Table 4.7. LULC changes in Kuala Lumpur Metropolitan Area (2001–2014).

	2001		2014		Net Changes (2001–2014)	
	ha ('000)	% of total	ha ('000)	% of total	ha ('000)	% of 2001
Urban Dense	34.56	3.45	55.22	5.52	20.66	59.77
Urban Sparse	121.34	12.13	213.88	21.37	92.54	76.26
Forest	468.94	46.86	368.21	36.80	-100.72	-21.48
Cropland	142.02	14.19	90.39	9.03	-51.63	-36.35
Grassland	130.14	13.00	130.50	13.04	0.36	0.28
Bareland	31.84	3.18	23.01	2.30	-8.84	-27.75
Water	64.46	6.44	63.90	6.39	-0.55	-0.86
Other land	7.40	0.74	55.59	5.55	48.19	651.23
Total	1000.70	100.00	1000.70	100.00		

4.8. Metro Manila, Philippines

Geographical and socioeconomic characteristics

Metropolitan Manila, commonly known as Metro Manila, is the center of the government, economy, education and culture of the Philippines. Composed of 16 cities and one municipality, including the City of Manila – the country's capital – Metro Manila has a total land area of 636 km^2, i.e. 0.2% of the country's land area. Geographically, Metro Manila is located at latitude 14° 35' North and longitude 121° 00' East, with Manila Bay in the western side and Laguna de Bay in the southeastern side. Among Metro Manila's 17 towns, Quezon City is the largest (171.71 km^2), while the smallest is San Juan (5.95 km^2). The governance of Metro Manila is exercised by the Metropolitan Manila Development Authority (MMDA).

Metro Manila is the country's largest manufacturing location and the second-largest employer after the wholesale and retail sectors (Lambino 2010). It also serves as the nation's principal port, with its excellent protected harbor (ADB 2014). The lands at the fringe of Metro Manila are in demand for residential subdivisions, sports and leisure centers, memorial parks and industrial complexes (Magno-Ballesteros 2000).

In 2000, Metro Manila had a population of 9.93 million (i.e. 12.98% of the country's population) and a density of 15,617.23 people/km^2, and in 2010 it had 11.86 million (i.e. 12.84% of the country's population) and 18,641.47 people/km^2, respectively (http://web0.psa.gov.ph). Metro Manila also exhibits the problems of many large cities, such as overpopulation, where local government struggles to keep up with the demand for services (ADB 2014). In addition, 31% of Metro Manila's land area is also flood prone, covering the cities of Manila, Navotas, Malabon and some parts of Caloocan (Magno-Ballesteros 2000).

LULC changes in Metro Manila

Figures 4.8(a) and 4.8(b) show the classified LULC maps of Metro Manila, while Figure 4.8(c) highlights the detected urban land changes between 2001 and 2014, including the changes from urban sparse to urban dense (red), non-urban to urban dense (blue) and non-urban to urban sparse (green). Due to the presence of the two main bodies of water (Manila Bay and Laguna de Bay), the spatial urban expansion of Metro Manila is mostly concentrated toward the north and south directions (Fig. 4.8). There are indications of urban sprawl as shown by the substantial urban land changes in the northern and southern parts. However, there are also signs of an infilling pattern as indicated by the urban land changes in the city center (Fig. 4.8).

In 2001, the area of urban dense was 27.57 thousand ha, accounting for 2.76% of the whole landscape (Table 4.8). In 2014, it increased to 49.80 thousand ha, i.e. 4.98% of the landscape, showing net increase of 80.67% from 2001. The increase in the area of urban dense was due to its gains from urban sparse and non-urban areas (Fig. 4.8(c)). Urban sparse also had a high net increase from 2001 to 2014 of 76.12%. In 2001, it had an area of 59.43 thousand ha (5.94%), which increased to 104.67 thousand ha in 2014 (10.47%) (Table 4.8). The increase in the area of urban sparse was at the expense of the other LULC classes (Fig. 8(c); Table 4.8).

Indeed, cropland had a net decrease of 10.75 thousand ha from 2001 to 2014 (-21.76%), while grassland had a net decrease of 82.02 thousand ha (-27.05%). Due to the presence of clouds and shadows, classified in this project as other land (Figs. 4.8(a) and 4.8(b)), it was not possible to ascertain the changes (gains and losses) in forest cover during the 2001–2014 period. However, there are indications that green spaces, including patches of forest, in the city center have been decreasing over the years. The details of the changes for the other LULC classes are summarized in Table 4.8. Overall, the data show that Metro Manila has experienced remarkable

landscape changes, especially in its fringe areas, posing many challenges in the context of landscape and urban planning for its sustainable urban development.

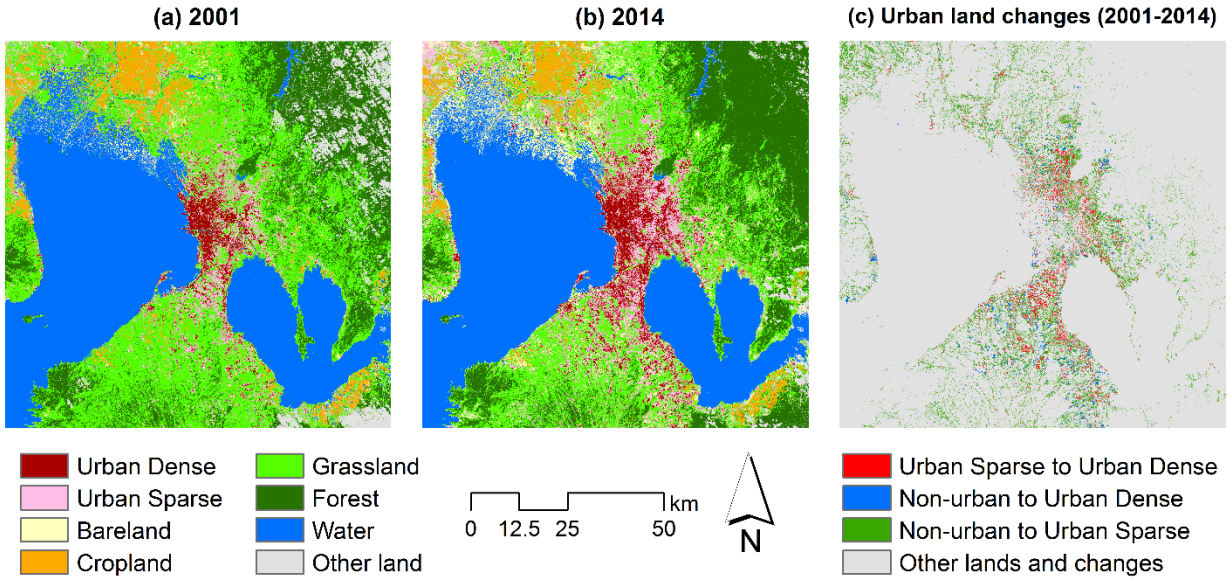

Fig. 4.8. LULC maps and spatial distribution of urban land changes in Metro Manila.

Table 4.8. LULC changes in Metro Manila (2001–2014).

	2001		2014		Net Changes (2001–2014)	
	ha ('000)	% of total	ha ('000)	% of total	ha ('000)	% of 2001
Urban Dense	27.57	2.76	49.80	4.98	22.24	80.67
Urban Sparse	59.43	5.94	104.67	10.46	45.24	76.12
Forest	156.63	15.66	190.99	19.09	34.37	21.94
Cropland	49.40	4.94	38.65	3.86	-10.75	-21.76
Grassland	303.26	30.31	221.24	22.11	-82.02	-27.05
Bareland	16.91	1.69	57.21	5.72	40.30	238.37
Water	337.40	33.73	322.75	32.26	-14.65	-4.34
Other land	49.81	4.98	15.08	1.51	-34.72	-69.72
Total	1000.40	100.00	1000.40	100.00		

4.9. Seoul Metropolitan Area, South Korea

Geographical and socioeconomic characteristics

The Seoul Capital Area (SCA) is the metropolitan area of South Korea and is commonly referred to as the Sudogwon or Gyeonggi region. It includes three different administrative districts, namely Incheon, Seoul and Gyeonggi-do. Seoul is the capital city. Geographically, it is located at latitude 37° 32′ North and longitude 127° 00′ East and is situated in the northwestern part of South Korea, near the Yellow Sea and the border of North Korea. The SCA covers a wide relatively flat land around the Han River valley. The total land area of Seoul metropolitan area is about 11,704 km^2, and Seoul city has an area of about 605 km^2.

The Seoul metropolitan area had a population of 21 million in 2000, representing 46% of the country's population (ADB 2014). The UN ranked Seoul as the 29th largest population agglomeration in the world in 2014; in 1990, it was ranked 9th (UN 2014). The population growth rate (0.11% from 2011 to 2014) started to decline in Seoul from 2011 (http://worldpopulationreview.com).

Today, the Seoul industrial sector has changed from the traditional labor-intensive manufacturing to information technology, electronics and assembly-type industries. Seoul is considered one of the leading and rising global cities. However, the higher level of industrialization, high consumerism, lack of available land and rapid urbanization contribute to the environmental problems in the SCA area.

LULC changes in Seoul Metropolitan Area

Figures 4.9(a) and 4.9(b) show the LULC classification results for Seoul using the maximum likelihood supervised classification method. Figure 4.9(c) highlights the detected LULC changes from non-urban to urban sparse (green), non-urban to urban dense (blue), urban sparse to urban dense (red) and other lands and changes (gray) between 2000 and 2014. A large area of urban dense is located on both sides of the main river, passing through the city. Many industries and administrative centers are located on the main riverbanks. In addition, urban dense and urban sparse are also highly concentrated in areas close to the sea. It can also be observed that vast forest areas surround the urban area. Cropland is also mixed with urban land use and forest area.

The area of urban dense was 31.63 thousand ha in 2000, covering 3.16% of the whole landscape (Table 4.9). In 2014, it increased to 84.70 thousand ha, i.e. 8.47% of the landscape, showing a net increase of 167.81% from 2000. The area of urban sparse in 2000 was 65.29 thousand ha (6.53%). In 2014, it increased to 201.40 thousand ha (20.13%), with a remarkable net increase of 208.48% from 2000.

Furthermore, the area of cropland was 298.44 thousand ha (29.83%) in 2000 and 214.96 thousand ha (21.49%) in 2014. The area of forest was 360.18 thousand ha (36%) in 2000 and 357.47 thousand ha (35.73%) in 2014. The net decrease in the area of grassland from 2000 to 2014 was substantial (-94.20% or 90.80 thousand ha). The details of the changes for the LULC classes are summarized in Table 4.9. Overall, the LULC changes in Jakarta metropolitan area show a great urban expansion, as indicated by the increase in the area of urban dense, but more especially that of urban sparse.

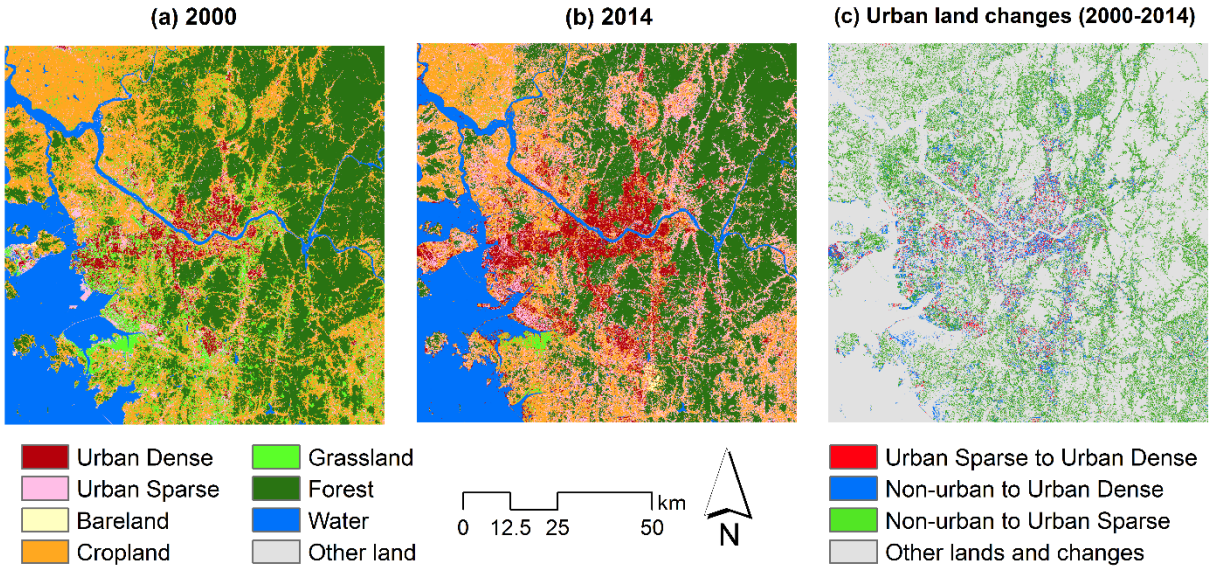

Fig. 4.9. LULC maps and spatial distribution of urban land changes in Seoul Metropolitan Area.

Table 4.9. LULC changes in Seoul Metropolitan Area (2000–2014).

	2000		2014		Net Changes (2000–2014)	
	ha ('000)	% of total	ha ('000)	% of total	ha ('000)	% of 2000
Urban Dense	31.63	3.16	84.70	8.47	53.07	167.81
Urban Sparse	65.29	6.53	201.40	20.13	136.11	208.48
Forest	360.18	36.00	357.47	35.73	-2.70	-0.75
Cropland	298.44	29.83	214.96	21.49	-83.48	-27.97
Grassland	96.39	9.64	5.59	0.56	-90.80	-94.20
Bareland	2.15	0.21	2.42	0.24	0.27	12.78
Water	146.33	14.63	133.85	13.38	-12.47	-8.53
Other land	0.00	0.00	0.00	0.00	0.00	---
Total	1000.40	100.00	1000.40	100.00		

4.10. Taipei Metropolitan Area, Taiwan

Geographical and socioeconomic characteristics

The Taipei–Keelung metropolitan area or the Greater Taipei area is the largest metropolitan area in Taiwan. Geographically, Taipei is located at latitude 25° 5' North and longitude 121° 33' East. The Taipei metropolitan area covers Taipei City, New Taipei City and Keelung City. The total land area of Taipei metropolitan area is about 2457 km^2, while Taipei City has an area of about 271 km^2. Taipei City is situated in a basin of northern Taiwan, and includes the hilly areas in the northeast and southeast sides of the city. The generally low-lying terrain covers the western side. The elevation in the hilly areas in the northeastern and southeastern sides in the Cising mountain area reaches up to 1120 m above sea level.

The estimated population of Taipei metropolitan area was 7,028,583 in 2014 (http://www.demographia.com), i.e. approximately 30.04% of the total population of Taiwan. In 2013, the population density of Taipei was 9,884 people/km^2. As the center of Taiwan's economy, Taipei experienced a rapid economic development over the years and became a leading high-technology producer. The rapid economic growth of Taipei over the past few decades has resulted in the expansion of urban areas and high rates of per capita consumption. The main economic goods produced in the metropolitan area include electronic products and components, electrical machinery and equipment, printed materials, precision equipment, foods and beverages and textiles.

LULC changes in Taipei Metropolitan Area

Figures 4.10(a) and 4.10(b) show the LULC classification results for Taipei using the maximum likelihood supervised classification method. Figure 4.10(c) highlights the detected LULC changes from non-urban to urban sparse (green), non-urban to urban dense (blue), urban sparse to urban dense (red) and other lands and changes (gray) between 2001 and 2014. The urban land use is mainly concentrated in the basin area of the major river. The southern part of the city is mostly covered with forest and the southwestern part is dominated by cropland. Urban dense and urban sparse are also observed in the coastal areas. The new port area can be identified in the LULC classification of 2014. The spatial pattern of urban sparse follows the road networks, which connect major urban dense areas.

The area of urban dense was 29.19 thousand ha in 2001, covering 2.92% of the whole landscape (Table 4.10). In 2014, it increased to 42.38 thousand ha, i.e. 4.24% of the landscape, showing a net increase of 45.20% from 2001. The area of urban sparse in 2001 was 85.43 thousand ha (8.54%). In 2014, it increased to 89.69 thousand ha (8.96%), with a net increase of 4.98% from 2001. Furthermore, the area of cropland was 35.42 thousand ha (3.54%) in 2001 and 45.87 thousand ha (4.59%) in 2014. The area of forest was 329.54 thousand ha (32.94%) in 2001 and 328.43 thousand ha (32.83%) in 2014. The net decrease in the area of grassland from 2001 to 2014 was substantial (-40.63% or 18.14 thousand ha). The details of the changes for the LULC classes are summarized in Table 4.10. Overall, the LULC changes in Taipei metropolitan area show that Taipei's urban has also been expanding, with the area of all other LULC classes declining, except for cropland.

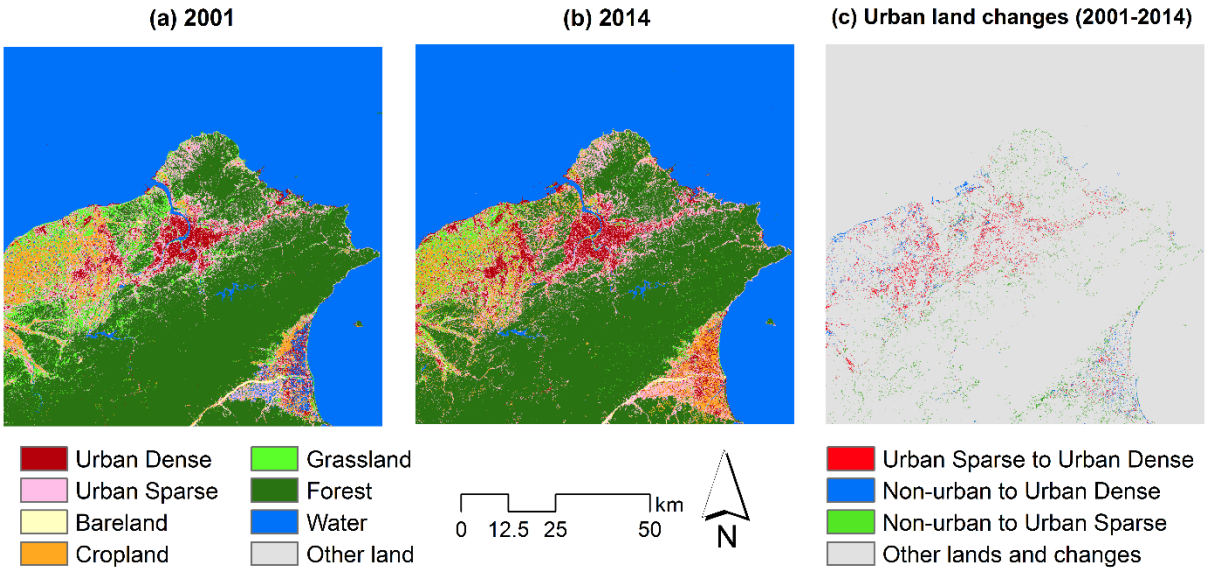

Fig. 4.10. LULC maps and spatial distribution of urban land changes in Taipei Metropolitan Area.

Table 4.10. LULC changes in Taipei Metropolitan Area (2001–2014).

	2001		2014		Net Changes (2001–2014)	
	ha (‘000)	% of total	ha (‘000)	% of total	ha (‘000)	% of 2001
Urban Dense	29.19	2.92	42.38	4.24	13.19	45.20
Urban Sparse	85.43	8.54	89.69	8.96	4.26	4.98
Forest	329.54	32.94	328.43	32.83	-1.11	-0.34
Cropland	35.42	3.54	45.87	4.59	10.45	29.49
Grassland	44.65	4.46	26.51	2.65	-18.14	-40.63
Bareland	1.79	0.18	1.56	0.16	-0.24	-13.18
Water	474.38	47.42	465.96	46.58	-8.41	-1.77
Other land	0.00	0.00	0.00	0.00	0.00	---
Total	1000.40	100.00	1000.40	100.00		

4.11. Tehran Metropolitan Area, Iran

Geographical and socioeconomic characteristics

Tehran is a mountainside city situated at an altitude of 900 to 1700 m above sea level. It covers an area of 1500 km^2 located on the slope of the Alborz Mountain. Its urban area spreads entirely over the Iranian plateau, on the slopes of a very high and dense mountain barrier, with a peak of 3933 m (better known as Towchal), which is 2200 m higher than the city's residential areas (http://en.tehran.ir).

As the capital city of Iran, Tehran has the largest population in the country and is the center of cultural, economic, political and social activities. According to the census data, Tehran's population increased from 6,758,845 to 8,154,051 from 1996 to 2011 (http://www.citypopulation.de). About 30% of Iran's public-sector workforce and 45% of large industrial firms are located in Tehran.

LULC changes in Tehran Metropolitan Area

Figures 4.11(a) and 4.11(b) show the LULC classification results for Tehran using the maximum likelihood supervised classification method. Figure 4.11(c) highlights the detected LULC changes from non-urban to urban sparse (green), non-urban to urban dense (blue), and urban sparse to urban dense (red) between 2000 and 2014. The gray areas are other lands and changes.

Table 4.11 shows the statistics of LULC changes between 2000 and 2014 in Tehran. The category "other land" refers to cloud and shadow. More specifically, the area and percentage of each LULC class, including the detected net changes are summarized in Table 4.11. Figures 4.11(a) and 4.11(b) clearly show the LULC characteristics of Tehran. Since Tehran has a dry climate, bareland is the dominant LULC type and water covers only a small area. The central area is dominated by urban dense and urban sparse and they stretch along the roads toward the west, southwest and southeast directions. The north side of Tehran is almost bareland because of the Alborz Mountain. Cropland and grassland are found in areas close to local people's residential areas (urban dense or urban sparse).

Table 4.11 shows a 71.35% and 368.52% net increase in the area of urban dense and urban sparse, respectively, from 2000 to 2014. Although it had a substantial increase over the past 14 years, the area of urban sparse is still small when compared with the whole study area (3.96%). The dominant LULC type, bareland, covers around 70% of the study area. The decrease in the area of bareland and cropland from 2000 to 2014 was due to urban expansion. The results also show that the area of grassland and forest increased during the same period. The said increase might have been influenced by seasonal differences between the two imageries used. Water only occupies around 0.1% of the whole area, indicating a water shortage problem in Tehran.

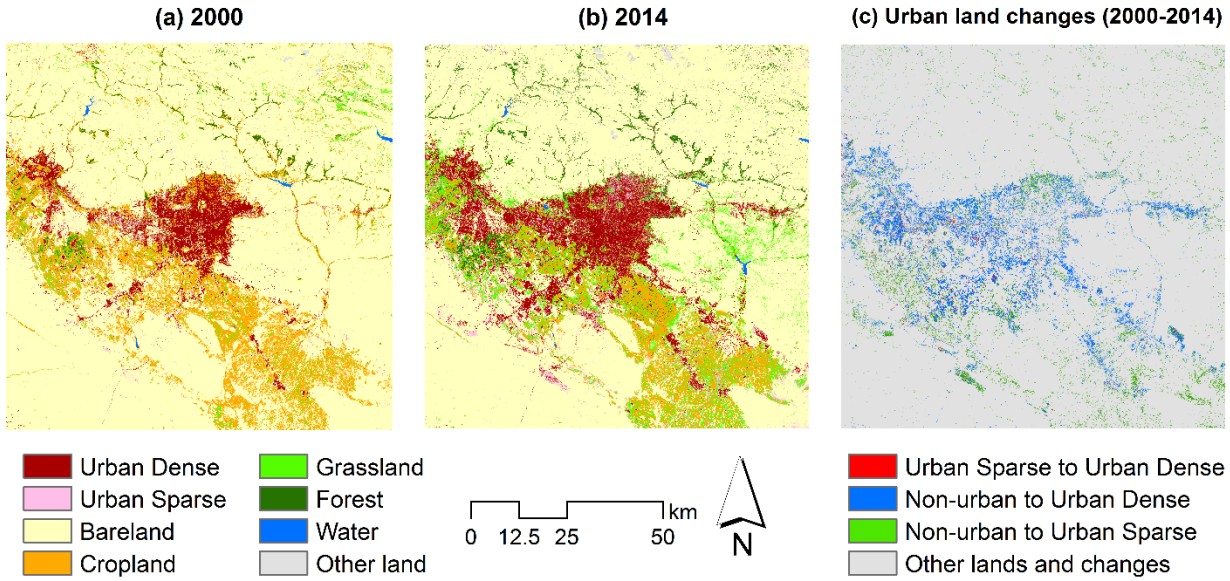

Fig. 4.11. LULC maps and spatial distribution of urban land changes in Tehran Metropolitan Area.

Table 4.11. LULC changes in Tehran Metropolitan Area (2000–2014).

	2000		2014		Net Changes (2000-2014)	
	ha ('000)	% of total	ha ('000)	% of total	ha ('000)	% of 2000
Urban Dense	52.48	5.24	89.92	8.99	37.44	71.35
Urban Sparse	8.46	0.85	39.64	3.96	31.18	368.52
Forest	9.84	0.98	24.37	2.44	14.53	147.60
Cropland	123.58	12.35	72.31	7.23	-51.27	-41.48
Grassland	24.02	2.40	74.57	7.45	50.56	210.50
Bareland	777.59	77.70	693.96	69.35	-83.63	-10.75
Water	1.12	0.11	1.18	0.12	0.06	5.47
Other land	3.61	0.36	4.74	0.47	1.13	31.34
Total	1000.70	100.00	1000.70	100.00		

4.12. Bamako Metropolitan Area, Mali

Geographical and socioeconomic characteristics

Bamako is the capital and largest city of the Republic of Mali. Geographically, Bamako is located at latitude 12° 37' North and longitude 8° 1' West. It is situated on both sides of the Niger River. The topography of Bamako is relatively flat except to the immediate north. The average elevation of the area is 350 m above sea level. A large area around Bamako City is covered by desert or semi-desert land. The development of Bamako City started in the northern part of the river, and later it was transferred to the southern part, following the construction of bridges.

Bamako is the seventh largest West African urban center after Lagos, Abidjan, Kano, Ibadan, Dakar and Accra. The area of the city is about 252 km^2. The population of Bamako City was 2.04 million in 2011, with an annual population growth rate of about 5.4%. In 2009, the population density of Bamako was 7,184 inhabitants/km^2 (http://www.citypopulation.de). The rapid population growth of Bamako has had a negative impact on the growing inadequacy of basic services, the expansion of informal settlements, congestion in the city center and increased pollution. Bamako is the major administrative center of Mali where major financial and trade activities are concentrated. Other economic activities in the city include farming (agriculture) and fishing (fishery).

LULC changes in Bamako Metropolitan Area

Figures 4.12(a) and 4.12(b) show the LULC classification results for Bamako using the maximum likelihood supervised classification method. Figure 4.12(c) highlights the detected LULC changes from non-urban to urban sparse (green), non-urban to urban dense (blue), urban sparse to urban dense (red) and other lands and changes (gray) between 1999 and 2014. In 1999, urban dense was mainly concentrated in the northern side of the river. However, in 2014, both the northern and southern sides of the river have been urbanized. While barelands surround the major urban area, croplands are found in areas much closer to the urban area.

In 1999, the area of urban dense was 0.65 thousand ha, covering 0.06% of the whole landscape (Table 4.12). In 2014, it increased to 6.33 thousand ha, i.e. 0.63% of the landscape, showing a net increase of 874.83% from 1999. The area of urban sparse area in 1999 was 23.59 thousand ha (2.36%), and in 2014, it increased to 53.30 thousand ha (5.33%). Furthermore, the area of cropland in 1999 was 11.24 thousand ha (1.12%), while in 2014, it increased to 15.36 thousand ha (1.54%). The area of forest also increased from 106.54 thousand ha (10.65%) in 1999 to 202.47 thousand ha (20.24%) in 2014. The details of the changes for the LULC classes are summarized in Table 4.12. Overall, the LULC changes in Bamako metropolitan area show a substantial urban expansion between 1999 and 2014, as indicated by the increase in the area of urban sparse, but more especially that of urban dense.

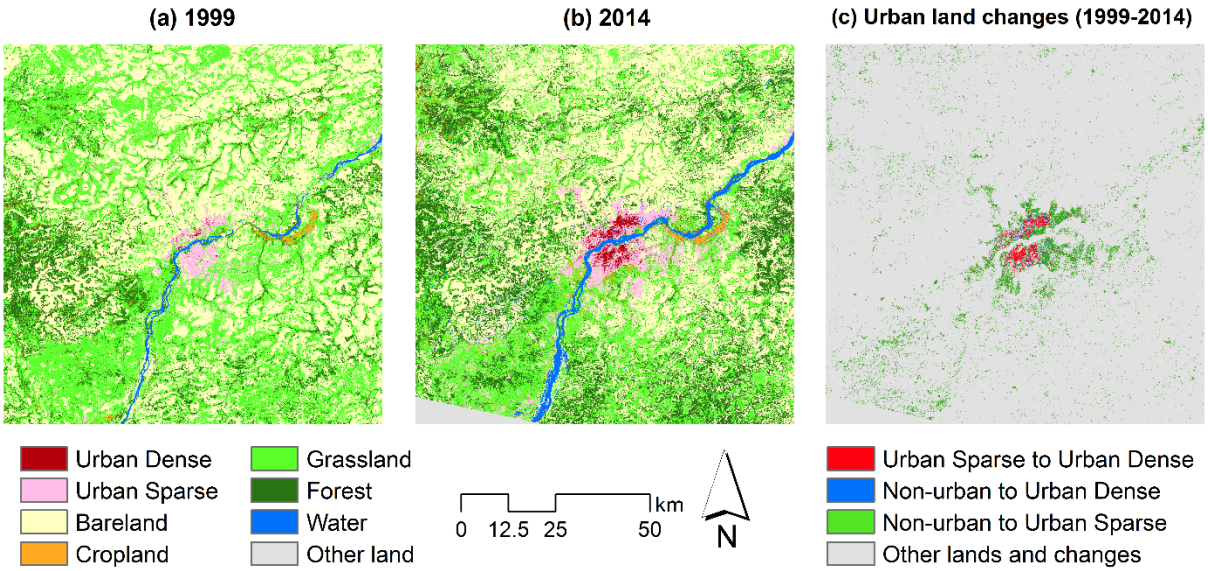

Fig. 4.12. LULC maps and spatial distribution of urban land changes in Bamako Metropolitan Area.

Table 4.12. LULC changes in Bamako Metropolitan Area (1999–2014).

	1999		2014		Net Changes (1999–2014)	
	ha ('000)	% of total	ha ('000)	% of total	ha ('000)	% of 1999
Urban Dense	0.65	0.06	6.33	0.63	5.68	874.83
Urban Sparse	23.59	2.36	53.30	5.33	29.71	125.91
Forest	106.54	10.65	202.47	20.24	95.93	90.04
Cropland	11.24	1.12	15.36	1.54	4.12	36.64
Grassland	401.44	40.13	285.83	28.57	-115.60	-28.80
Bareland	449.86	44.97	403.95	40.38	-45.92	-10.21
Water	7.07	0.71	20.97	2.10	13.90	196.56
Other land	0.00	0.00	12.18	1.22	12.18	---
Total	1000.40	100.00	1000.40	100.00		

4.13. Nairobi Metropolitan Area, Kenya

Geographical and socioeconomic characteristics

Nairobi is located in between Kampala and Mombasa. It has an area of 684 km^2. It lies adjacent to the eastern edge of the rift valley and is situated 1661 m above sea level (http://www.nairobi.com). The Ngong hills occupy the western part of the city. Mount Kenya is located north of Nairobi, while Mount Kilimanjaro lies on the southeastern side of the city. The Nairobi River, along with its tributaries, passes through Nairobi Province.

Nairobi, since its foundation in 1899, has grown to become the second largest city in the African Great Lakes, despite being one of the youngest cities in the region. According to the census data from the Kenya government, Nairobi's population increased from 2,143,254 to 3,133,518 at a rate of 3.87% per year from 1999 to 2009 (http://www.citypopulation.de). With this growth rate, Nairobi's population is expected to reach 5 million by 2025. The City Square is located in the heart of Nairobi, while the Kenyan Parliament buildings, Nairobi Law Courts, Kenyatta Conference Centre, the Holy Family Cathedral and the Nairobi City Hall surround the square.

LULC changes in Nairobi Metropolitan Area

Figures 4.13(a) and 4.13(b) show the LULC classification results for Nairobi using the maximum likelihood supervised classification method. Figure 4.13(c) highlights the detected LULC changes from non-urban to urban sparse (green), non-urban to urban dense (blue) and urban sparse to urban dense (red) between 2000 and 2014. The gray areas are other lands and changes.

Table 4.13 shows the statistics of LULC changes between 2000 and 2014 in Nairobi. The category "other land" refers to cloud and shadow. More specifically, the area and percentage of each LULC class, including the detected net changes are summarized in Table 4.13. It can be observed from Figures 4.13(a) and 4.13(b) that most of the LULC classes show a distinct spatial pattern. Urban dense and urban sparse both dominate the city proper, while cropland, grassland and forest dominate the northern and eastern parts of the city. The southern and western parts, where Ngong hills are located, are dominated by bareland. That said, the urban area, especially the urban dense, is very small. This is because the area of Nairobi City is small compared with the whole study area. Figure 4.13(c) shows that most of the gains of urban dense are found in the city proper, while the gains of urban sparse are relatively more scattered. This spatial pattern of the gains of urban sparse might have been influenced by the increasing number of small houses around the city proper.

Table 4.13 shows that the area of urban dense and urban sparse increased substantially by 124.38% and 219.69%, respectively, from 2000 to 2014. By contrast, except for water, the area of all the other LULC types decreased. All these changes give indications that indeed Nairobi has been experiencing a rapid urbanization. Cropland and grassland decreased by almost 25,000 and 15,000 ha, respectively, while bareland, the dominant LULC type in the area, only decreased by less than 5,000 ha. This indicates that most of the gains of urban dense and urban sparse came from the other LULC classes, including the valuable vegetated areas. The change in the area of water also needs to be mentioned because it increased by 33.86%. Normally the area of water does not change too much. But for the case of Nairobi, it was due to the ponds constructed after 2000.

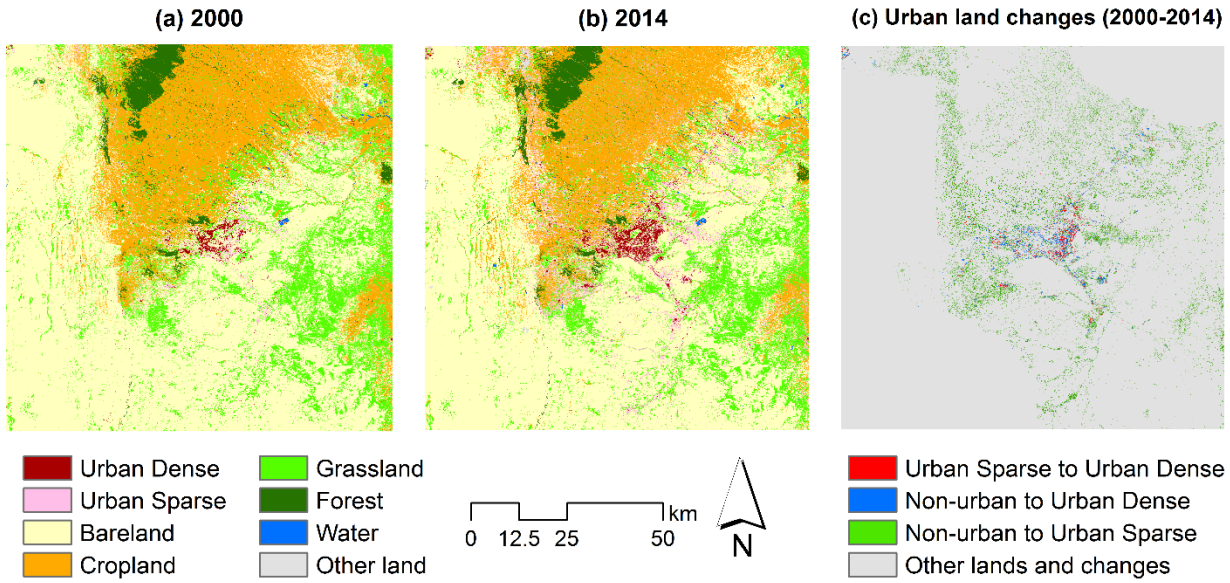

Fig. 4.13. LULC maps and spatial distribution of urban land changes in Nairobi Metropolitan Area.

Table 4.13. LULC changes in Nairobi Metropolitan Area (2000–2014).

	2000		2014		Net Changes (2000–2014)	
	ha ('000)	% of total	ha ('000)	% of total	ha ('000)	% of 2000
Urban Dense	5.24	0.52	11.75	1.17	6.51	124.38
Urban Sparse	16.00	1.60	51.15	5.11	35.15	219.69
Forest	30.57	3.06	29.78	2.98	-0.79	-2.60
Cropland	219.03	21.89	194.71	19.46	-24.32	-11.11
Grassland	151.97	15.19	137.39	13.73	-14.58	-9.59
Bareland	576.29	57.61	571.92	57.17	-4.37	-0.76
Water	1.30	0.13	1.74	0.17	0.44	33.86
Other land	0.00	0.00	1.97	0.20	1.97	---
Total	1000.40	100.00	1000.40	100.00		

5. Summary

LULC mapping is an important component of the practical applications of remote sensing technology. LULC maps can be used for various purposes in the realms of sustainability, global environmental change, landscape ecology, and urban and geographical studies. Furthermore, remote sensing-derived LULC maps are of particular importance to the developing countries, where the availability of multi-temporal and spatially consistent LULC maps is still limited.

As part of the ongoing effort to establish a database of remote sensing-derived LULC maps, the LULC maps of 11 major Asian cities and two major African cities for the 2000 and 2014 epochs have been classified from remote sensing satellite imageries (Landsat imageries). The classified LULC maps, including some descriptions and analyses of the detected LULC changes for each city, have been presented in this report (Sections 4.1–4.13).

Figure 5.1 presents a summary of the LULC classification and change detection results, highlighting (a) the density of total built-up lands (urban dense + urban sparse) in 2000 and 2014 epochs, and (b) the percentage increase of total built-up lands (2000–2014) for the 13 major cities. Based on the 100 km × 100 km landscape unit of analysis, it can be observed that in the 2000 epoch, Beijing had the highest built-up density with 32.55%, while Dhaka had the lowest with 2.07% (Fig. 5(a)). In the 2014 epoch, Beijing still had the highest with 49.47%, while Kathmandu had the lowest with 4.97%. In terms of percentage increase from 2000 to 2014, Dhaka had the highest with 251.21%, while Taipei had the lowest with 15.18% (Fig. 5(b)).

Among the three megacities of Southeast Asia (i.e. Bangkok, Jakarta and Manila), Bangkok had the highest built-up density in both epochs (13.57% and 21.84%), followed by Jakarta (8.97% and 16.19%) and Manila (8.70% and 15.44%) (Fig. 5(a)). However, in terms of percentage increase, Jakarta had the highest with 80.50%, followed by Manila (77.47%) and Bangkok (60.94%) (Fig. 5(b)). While the two African cities (i.e. Bamako and Nairobi) are among those cities with low built-up density for both epochs, they both had high percentage increase: Nairobi is the second highest with 196.23%, while Bamako comes fourth with 146.28%. This indicates that, like most of Asian cities, African cities have also been experiencing rapid urbanization.

In this project, we acknowledge that the LULC classification process has been very challenging due to some technical issues such as seasonal differences in the imageries used, presence of clouds, shadows and snows (in Kathmandu), spectral confusion between classes (e.g. between urban dense, urban sparse, cropland and bareland (including coastal sand dunes, river wash and exposed mountain rocks); between cropland and grassland; between grassland and forest; and between water channels and roads), as well as the inherent complex nature of each city's landscape pattern. Nevertheless, though the respective quantitative accuracy of the classified LUC maps is yet to be assessed, we paid careful attention to these issues during the classification process, with the aim of producing accurate LULC maps. A part of the future plan for this project is to expand the 13 sites by including more Asian and African cities. The experience and lessons we gained and learned from the 13 major cities, particularly in the processing of the remote sensing satellite imageries and interpretation of the data, will be used in the future endeavors of this project.

Some of the LULC maps (Figs. 4.1–4.13) have been uploaded in a WebGIS (http://land.geo.tsukuba.ac.jp/geovisualization), designed and developed for the purpose of visualizing the urban land changes in the 13 major cities.

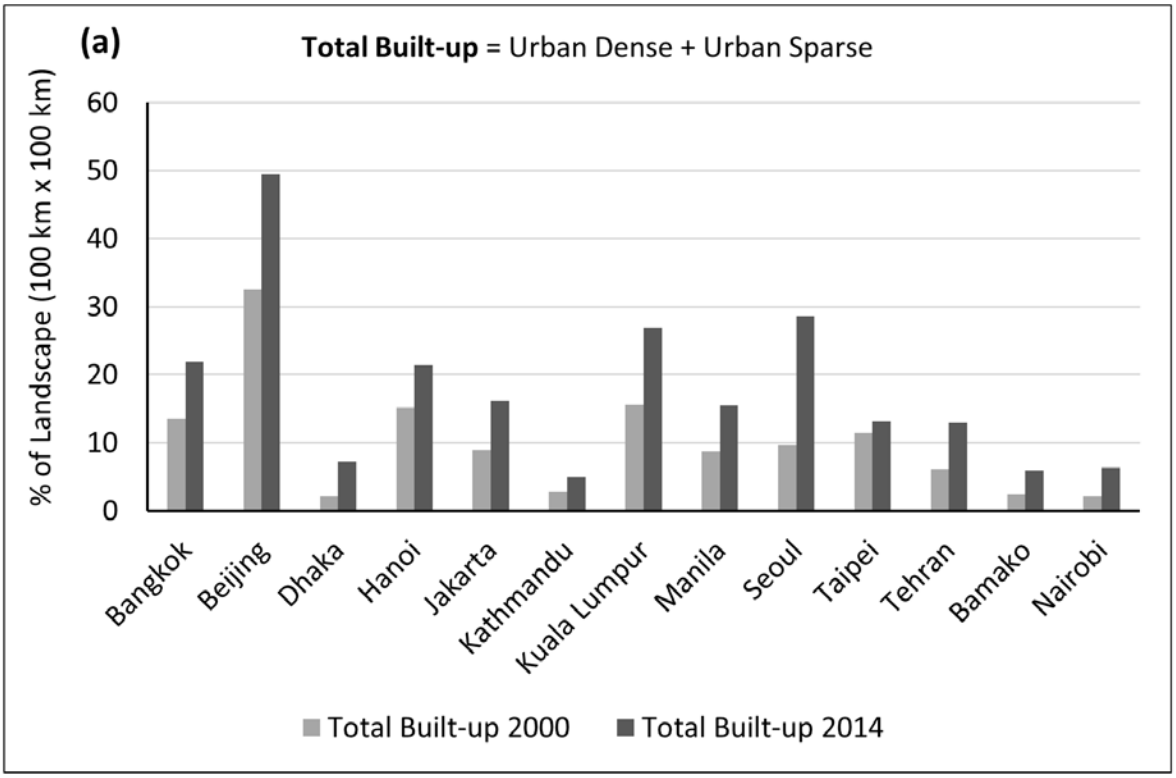

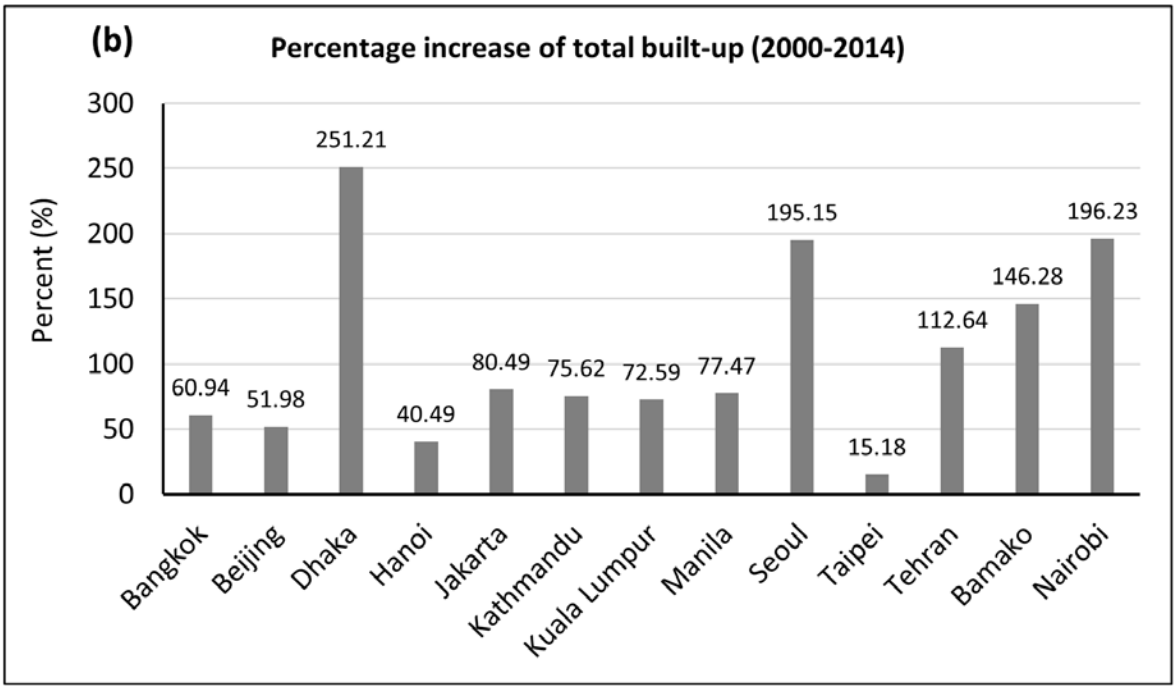

Fig. 5. Summary of the LUC classification and change detection results, highlighting (a) the density of total built-up lands (urban dense + urban sparse) in the 2000 and 2014 epochs, and (b) the percentage increase of total built-up lands (2000–2014).

Acknowledgements

The construction of the land-use/land-cover database is financially supported by the Data Bank Project, University of Tsukuba (Representative: Kazuo Kishimoto). The spatial analysis of the database is supported by Grant-in-Aid for Scientific Research A (No. 24241053, 2013-16, Representative: Tsutomu Suzuki) and B (No. 26284129, 2014-16, Representative: Yuji Murayama). The second author (Ronald C. Estoque) is supported by the JSPS, under the grant for postdoctoral fellowship.

References

Abtew, W. & Melesse, A. 2012. *Evaporation and evapotranspiration: measurements and estimations*. New York: Springer.

ADB. 2014. *Urban metabolism of six Asian cities.* Mandaluyong City, Philippines: Asian Development Bank.

Akar, O. & Gungor, O. 2012. Classification of multispectral images using Random Forest algorithm. *Journal of Geodesy and Geoinformation 1*, 105–112.

Akbari, H., Shea, R.L. & Taha, H. 2003. Analyzing the land cover of an urban environment using high resolution orthophotos. *Landscape and Urban Planning 63*, 1–14.

Anderson, J.R. 1976. A land use and land cover classification system for use with remote sensor data. Washington, US Government Printing Office.

Anderson, L.O., Malhi, Y., Aragão, L.E., Ladle, R., Arai, E., Barbier, N. & Phillips, O. 2010. Remote sensing detection of droughts in Amazonian forest canopies. *New Phytologist 187*, 733–750.

Angel, S., Parent, J., Civco, D.L., Alejandro M. & Blei, A.M. 2012. *Atlas of urban expansion.* Cambridge MA: Lincoln Institute of Land Policy.

Aronoff, S. 2005. *Remote sensing for GIS managers*. Redlands, CA: ESRI Press.

Arsanjani, J.J., Helbich, M. & Vaz, E.D. 2013. Spatiotemporal simulation of urban growth patterns using agent-based modeling: the case of Tehran. *Cities 32*, 33–42.

Aspinall, R. 2006. Editorial. *Journal of Land Use Science 1*, 1–4. Bagan, H. & Yamagata, Y. 2014. Land-cover change analysis in 50 global cities by using a combination of Landsat data and analysis of grid cells. *Environmental Research Letters 9*, 064015.

Bellvert, J., Zarco-Tejada, P.J., Girona, J. & Fereres, E. 2013. Mapping crop water stress index in a 'Pinot-noir' vineyard: comparing ground measurements with thermal remote sensing imagery from an unmanned aerial vehicle. *Precision Agriculture*, 1–16.

Benediktsson, J.A., Pesaresi, M. & Amason, K. 2003. Classification and feature extraction for remote sensing images from urban areas based on morphological transformations. *IEEE Transactions on Geoscience and Remote Sensing 41*, 1940–1949.

Bergquist, R. 2011. New tools for epidemiology: a space odyssey. *Memórias do Instituto Oswaldo Cruz 106*, 892–900.

Blaschke, T. 2010. Object based image analysis for remote sensing. *ISPRS Journal of Photogrammetry and Remote Sensing 65*, 2–16.

Blaschke, T., Hay, G.J., Kelly, M., Lang, S., Hofmann, P., Addink, E., et al. 2014. Geographic object-based image analysis—towards a new paradigm. *ISPRS Journal of Photogrammetry and Remote Sensing 87*, 180–191.

Blaschke, T., Lang, S. & Möller, M. 2004. Object-based analysis of remote sensing data for landscape monitoring: recent developments. Anaix XII Simposio Brasileiro de Sensoriamento Remoto, Goiania, Brasil, 16–21 abril 2005. *INPE,* 2879–2885.

Breiman, L. 2001. Random forests. *Machine Learning 45*, 5–32.

Brian, W. S., Qi, C. & Michael, B. 2011. A comparison of classification techniques to support land cover and land use analysis in tropical coastal zones. *Applied Geography 31*(2), 525–532.

Chan, J.C.W., Chan, K.P. & Yeh, A.G.O. 2001. Detecting the nature of change in an urban environment: a comparison of machine learning algorithms. *Photogrammetric Engineering and Remote Sensing 67*, 213–225.

Chen, X.L., Zhao, H.M., Li, P.X. & Yin, Z.Y. 2006. Remote sensing image-based analysis of the relationship between urban heat island and land use/cover changes. *Remote Sensing of Environment 104*, 133–146.

Chopra, R., Verma, V.K. & Sharma, P.K. 2001. Mapping, monitoring and conservation of Harike wetland ecosystem, Punjab, India, through remote sensing. *International Journal of Remote Sensing 22*, 89–98.

Chowdhury, M.S.A. 2007. Good governance and urbanization for promotion of sustainable development in Bangladesh. In: Maiti, E.P. (Eds.). *Development studies (Vol. 1)*. Atlantic Publishers.

Dadras, M., Mohd Shafri, H.Z., Ahmad, N., Pradhan, B. & Safarpour, S. 2014. Land use/cover change detection and urban sprawl analysis in Bandar Abbas City, Iran. *The Scientific World Journal*, 12–16.

Dalsted, K., Paris, J.F., Clay, D.E., Clay, S.A., Reese, C.L. & Chang, J. 2003. Selecting the appropriate satellite remote sensing product for precision farming. *POTASH & PHOSPHATE INSTITUTE. Site specific management guidelines. Georgia 40.*

Estoque, R.C. & Murayama, Y. 2011. Spatio-temporal urban land use/cover change analysis in a hill station: the case of Baguio City, Philippines. *Procedia-Social and Behavioral Sciences 21*, 326–335.

Estoque, R.C. & Murayama, Y. 2012. Examining the potential impact of land use/cover changes on the ecosystem services of Baguio city, the Philippines: a scenario-based analysis. *Applied Geography 35*, 316–326.

Estoque, R.C. & Murayama, Y. 2013a. City profile: Baguio. *Cities 30*, 240–251.

Estoque, R.C. & Murayama, Y. 2013b. Landscape pattern and ecosystem service value changes: implications for environmental sustainability planning for the rapidly urbanizing summer capital of the Philippines. *Landscape and Urban Planning 116*, 60–72.

Estoque, R.C., Murayama, Y., Kamusoko, C. & Yamashita, A. 2014. Geospatial analysis of urban landscape patterns in three major cities of Southeast Asia. *Tsukuba Geoenvironmental Sciences 10*, 3–10.

Fang, H. 1998. Rice crop area estimation of an administrative division in China using remote sensing data. *International Journal of Remote Sensing 19*, 3411–3419.

Ferencz, C., Bognar, P., Lichtenberger, J., Hamar, D., Tarcsai, G., Timar, G., et al. 2004. Crop yield estimation by satellite remote sensing. *International Journal of Remote Sensing 25*, 4113–4149.

Goodchild, M.F. 1994. Integrating GIS and remote sensing for vegetation analysis and modeling: methodological issues. *Journal of Vegetation Science 5*, 615–626.

Griffiths, P., Hostert, P., Gruebner, O. & van der Linden, S. 2010. Mapping megacity growth with multi-sensor data. *Remote Sensing of Environment 114*, 426–439.

Gutman, G., Janetos, A.C., Justice, C.O., Moran, E.F., Mustard, J.F., Rindfuss, R.R., et al. (Eds.). 2004. *Land change science: Observing, monitoring and understanding trajectories of change on the Earth's surface.* New York: Kluwer Academic.

Haregeweyn, N., Fikadu, G., Tsunekawa, A., Tsubo, M. & Meshesha, D.T. 2012. The dynamics of urban expansion and its impacts on land use/land cover change and small-scale farmers living near the urban fringe: a case study of Bahir Dar, Ethiopia. *Landscape and Urban Planning 106*, 149–157.

Hay, G.J. & Castilla, G. 2008. Geographic object-based image analysis (GEOBIA): a new name for a new discipline. In: Blaschke, T., Lang, S. & Hay, G.J. (Eds.). *Object based image analysis.* Heidelberg, Berlin, New York: Springer, 93–112.

Hewitt, R. & Escobar, F. 2011. The territorial dynamics of fast-growing regions: unsustainable land use change and future policy challenges in Madrid, Spain. *Applied Geography 31*, 650–667.

Hüttich, C., Herold, M., Wegmann, M., Cord, A., Strohbach, B., Schmullius, C. & Dech, S. 2011. Assessing effects of temporal compositing and varying observation periods for large-area land-cover mapping in semi-arid ecosystems: implications for global monitoring. *Remote Sensing of Environment 115*, 2445–2459.

JAXA. 2008. *ALOS data users handbook: revision C*. Earth Observation Research and Application Center, Japan Aerospace Exploration Agency (JAXA), Japan.

Lambin, E.F. & Ehrlich, D.1997. Land-cover changes in sub-Saharan Africa (1982–1991): application of a change index based on remotely sensed surface temperature and vegetation indices at a continental scale. *Remote Sensing of Environment 61*, 181–200.

Lambin, E.F., Turner, B.L., Geist, H.J., Agbola, S.B., Angelsen, A., Bruce, J.W., et al. 2001. The causes of land-use and land-cover change: moving beyond the myths. *Global Environmental Change 11*, 261–269.

Lambin.E.F., Geist, H.J. & Rindfuss, R.R. 2006. Introduction: local processes with global impacts. In: Lambin, E.F. & Geist, H.J. (Eds.). *Land-use and land-cover change: local processes and global impacts*. Heidelberg, Berlin, Germany: Springer, 1–8.

Lambino, J. 2010. The economic role of Metro Manila in the Philippines: A study of uneven regional development under globalization. *The Kyoto Economic Review 79*, 156–195.

Liaw, A. & Wiener, M. 2002. Classification and regression by RandomForest. *R News 2*, 18–22.

Lwin, K.K., Estoque, R.C. & Murayama, Y. 2012. Data collection, processing, and applications for geospatial analysis. In: Murayama, Y. Ed. *Progress in geospatial analysis*. Tokyo: Springer, 29–48.

Lwin, K.K. & Murayama, Y. 2013. Evaluation of land cover classification based on multispectral versus pansharpened landsat ETM+ imagery. *GIScience & Remote Sensing 50*, 458–472.

Magno-Ballesteros, M. 2000. Land use planning in Metro Manila and the urban fringe: implications on the land and real estate market. Philippine Institute for Development Studies, Discussion Paper Series No. 2000-20. Makati City, Philippines: PIDS.

Moghadam, S.H. & Helbich, M. 2013. Spatiotemporal urbanization processes in the megacity of Mumbai, India: a Markov chains-cellular automata urban growth model. *Applied Geography 40*, 140–149.

Moran, M.S., Inoue, Y. & Barnes, E.M.1997.Opportunities and limitations for image-based remote sensing in precision crop management. *Remote Sensing of Environment 61*, 319–346.

Morel, A.C., Saatchi, S.S., Malhi, Y., Berry, N.J., Banin, L., Burslem, D., et al. 2011. Estimating aboveground biomass in forest and oil palm plantation in Sabah, Malaysian Borneo using ALOS PALSAR data. *Forest Ecology and Management 262*, 1786–1798.

Müller, D. & Munroe, D.K. 2014. Current and future challenges in land-use science. *Journal of Land Use Science 9*, 133–142.

Mundia, C.N., Aniya, M. & Murayama Y. 2011. Modeling of spatial processes of urban growth in an African City. In: Kamusoko, C., Mundia. C.N. & Murayama.Y. (Eds.). *Recent advances in GIS and remote sensing analysis in Sub-Sahara Africa.* NOVA Science Publishers, 5–22.

Nelson, E., Mendoza, G., Regetz, J., Polasky, S., Tallis, H., Cameron, D., et al. 2009. Modeling multiple ecosystem services, biodiversity conservation, commodity production, and tradeoffs at landscape scales. *Frontiers in Ecology and the Environment 7*, 4–11.

Pareta, K. & Pareta, U. 2011. Forest carbon management using satellite remote sensing techniques: a case study of Sagar district (MP). *International Scientific Research Journal 3*, 335–348.

Phinn, S.R., Menges, C., Hill, G.J. & Stanford, M. 2000. Optimizing remotely sensed solutions for monitoring, modeling, and managing coastal environments. *Remote Sensing of Environment 73*, 117–132.

Platt, R.V. & Rapoza, L. 2008. An evaluation of an object-oriented paradigm for land use/land cover classification. *The Professional Geographer 60*, 87–100.

Polasky, S., Nelson, E., Pennington, D. & Johnson, K.A. 2011. The impact of land-use change on ecosystem services, biodiversity and returns to landowners: a case study in the State of Minnesota. *Environmental and Resource Economics 48*, 219–242.

Powell, S.L., Pflugmacher, D., Cohen, W.B., Kirschbaum, A.A. & Kim, Y. 2007. Moderate resolution remote sensing alternatives: a review of Landsat-like sensors and their applications. *Journal of Applied Remote Sensing 1*, 012506.

Reenberg, A. 2009. Land system science: Handling complex series of natural and socio-economic processes. *Journal of Land Use Science 4*, 1–4.

Richards, J.A. 1993. *Remote sensing digital image analysis: an introduction.* New York: Springer-Verlag.

Rodriguez-Galiano, V.F., Ghimire, B., Rogan, J., Chica-Olmo, M. & Rigol-Sanchez, J.P. 2012. An assessment of the effectiveness of a random forest classifier for land-cover classification. *ISPRS Journal of Photogrammetry and Remote Sensing 67*, 93–104.

Rogan, J. & Chen, D. 2004. Remote sensing technology for mapping and monitoring land-cover and land-use change. *Progress in Planning 61*, 301–325.

Seto, K.C., Fragkias, M., Güneralp, B. & Reilly, M.K. 2011. A meta-analysis of global urban land expansion. *PloS One 6*, e23777.

Siemens. 2011. *Asian green city index. Assessing the environmental performance of Asia's major cities*. Munich, Germany.

Smith, A., Kolden, C.A., Tinkham, W.T., Talhelm, A.F., Marshall, J.D., Hudak, A.T., et al. 2014. Remote sensing the vulnerability of vegetation in natural terrestrial ecosystems. *Remote Sensing of Environment 154*, 319–321.

Sohl, T. & Sleeter, B.2011.Role of remote sensing for land-use and land-cover change modelling. In: Giri, C.P. (Ed.). *Remote sensing of land use and land cover: principles and applications*. Boca Raton: CRC Press.

Stow, D.A., Hope, A., McGuire, D., Verbyla, D., Gamon, J., Huemmrich, F., et al. 2004. Remote sensing of vegetation and land-cover change in Arctic Tundra Ecosystems. *Remote Sensing of Environment 89*, 281–308.

Thapa, R. B. & Murayama, Y. 2012a. Scenario-based urban growth allocation in Kathmandu Valley, Nepal. *Landscape and Urban Planning 105*, 140–148.

Thapa. R.B. & Murayama.Y. 2012b. Urban growth modeling using the Bayesian probability function. In: Murayama.Y. (Ed.). *Progress in geospatial analysis*, Tokyo: Springer, 197–214.

Thapa, R.B., Murayama,Y. & Ale, S. 2008. Kathmandu. *Cities 25*, 45–57.

Tong, L., Xu, X., Fu, Y. & Li, S. 2014. Wetland changes and their responses to climate change in the three-river headwaters: region of China since the 1990s. *Energies 7*, 2515–2534.

Townshend, J., Justice, C., Li, W., Gurney, C. & McManus, J.1991. Global land cover classification by remote sensing: present capabilities and future possibilities. *Remote Sensing of Environment 35*, 243–255.

Turner, I.I. & Meyer, W.B. 1994. Global land-use and land-cover change. In: Meyer, W.B. & Turner, I.I. (Eds.). *Changes in land use and land cover: a global perspective*. Cambridge University Press.

Turner II, B.L., Lambin, E.F. & Reenberg. A. 2007.The emergence of land change science for global environmental change and sustainability. *Proceedings of the National Academy of Sciences of the United States of America 104*, 20666–20671.UN (United Nations). 2014. *World urbanization prospects: the 2014 revision, highlights*. New York: UN.

Vapnik, V. 1995. *The nature of statistical leaning theory*. New York: Springer Verlag.

Verburg, P.H., Erb, K.H., Mertz, O. & Espindola, G. 2013. Land system science: Between global challenges and local realities. *Current Opinion in Environmental Sustainability 5*, 433–437.

Vimal, R., Geniaux, G., Pluvinet, P., Napoleone, C. & Lepart, J. 2012. Detecting threatened biodiversity by urbanization at regional and local scales using an urban sprawl simulation approach: application on the French Mediterranean region. *Landscape and Urban Planning 104*, 343–355.

World Bank. 2009. *Climate change impact and adaptation study for Bangkok Metropolitan Region.* The World Bank Group.

Yamashita, A. 2011. A comparative analysis on land use distributions and their changes in Asian mega cities. In: Taniguchi, M. (Ed.). *Groundwater and subsurface environments: human impacts in Asian coastal cities.* Tokyo: Springer, 61–81.

Yang, J., Weisberg, P.J. & Bristow, N.A. 2012. Landsat remote sensing approaches for monitoring long-term tree cover dynamics in semi-arid woodlands: comparison of vegetation indices and spectral mixture analysis. *Remote Sensing of Environment 119*, 62–71.

Web References

http://archive.today/toTM. Malaysia: largest cities and towns and statistics of their population. (Accessed: 20 January 2015).

http://archive.unu.edu. Economic structural change and urbanization. (Accessed: 20 January 2015).

http://asterweb.jpl.nasa.gov. ASTER Mission. (Accessed: 29 December 2014).

http://balita.ph. Vietnam's population soars. (Accessed: 20 January 2015).

http://bioval.jrc.ec.europa.eu. Global land cover 2000 database. European Commission, Joint Research Centre. (Accessed: 28 December 2014).

http://due.esrin.esa.int/globcover. European Space Agency GlobCover Portal. (Accessed: 19 January 2015).

http://earthexplorer.usgs.gov. Landsat archive. (Accessed: 10 September 2014).

http://en.tehran.ir. Tehran Municipality, Public & International Relations Department. Tehran: Environment & Geography. (Accessed: 9 January 2015).

http://english.mofcom.gov.cn. Ministry of Commerce People's Republic of China. Doing business in Beijing. (Accessed: 20 January 2015)

http://glcf.umd.edu/library/guide/QuickBird_Product_Guide.pdf. QuickBird product guide. (Accessed: 17 January 2015).

http://land.geo.tsukuba.ac.jp/geovisualization. Official website of the Geovizualization to Urbanization Project. Division of Spatial Information Science, University of Tsukuba, Japan.

http://landsat.usgs.gov/about_landsat5.php. Landsat 5 history. (Accessed: 17 January 2015).

http://landsat.usgs.gov/about_landsat7.php. Landsat 7 history. (Accessed: 17 January 2015).

http://landsat.usgs.gov/landsat8.php. Product information: Landsat 8 data. (Accessed: 6 January 2015).

http://modis.gsfc.nasa.gov. Images of the day – Hawaii. (Accessed: 19 January 2015).

http://modis.gsfc.nasa.gov/about/specifications.php. About MODIS: specifications. (Accessed: 17 January 2015).
http://noaasis.noaa.gov/NOAASIS/ml/avhrr.html. Advanced very high resolution radiometer – AVHRR. (Accessed: 5 January 2015).
http://sedac.ciesin.columbia.edu. Socioeconomic Data and Applications Center (SEDAC). (Accessed: 19 January 2015).
http://tuoitrenews.vn. Hanoi population management faces challenges. (Accessed: 20 January 2015).
http://web0.psa.gov.ph. Philippine Statistics Authority. (Accessed: 13 January 2015).
http://worldpopulationreview.com. World Population Review. (Accessed: 25 December 2014).
http://www.bbs.gov.bd/PageWebMenuContent.aspx?MenuKey=337. Bangladesh Population Census Report – 2001, Community Series. Dhaka. Bangladesh Bureau of Statistics, Bangladesh. (Accessed: 19 January 2015).
http://www.blackbridge.com/geomatics/upload/airbus/SPOT1-5%20Resolutions%20and%20Spectral%20Modes.pdf. SPOT 1-5. (Accessed: 18 January 2015).
http://www.citypopulation.de. City population. (Accessed: 9 January 2015).
http://www.cnes.fr/web/CNES-en/1415-spot.php. SPOT-Looking down on Earth. (Accessed: 18 January 2015).
http://www.dbkl.gov.my. Kuala Lumpur Structure Plan 2020. (Accessed: 20 January 2015).
http://www.demographia.com/db-worldua.pdf. Demographia world urban areas. (Accessed: 19 January 2015)
http://www.eorc.jaxa.jp/ALOS/en/about/about_index.htm. About ALOS-Overview and objectives. (Accessed: 17 January 2015).
http://www.glcn.org. Global Land Cover Network. (Accessed: 20 January 2015).
http://www.globallandcover.com. Open land sservice: global land cover mapping. (Accessed: 25 December 2014).
http://www.globaltimes.cn. Beijing population reaches 21 million. (Accessed: 20 January 2015).
http://www.gso.gov.vn. General Statistics Office of Vietnam. (Accessed: 20 January 2015).
http://www.kathmandu.gov.np. Kathmandu Metropolitan City Office. (Accessed: 9 January 2015).
http://www.lboro.ac.uk. Globalization and World Cities Research Network. (Accessed: 19 January 2015)
http://www.lincolninst.edu. Lincoln Institute of Land Policy. (Accessed: 23 December 2014).
http://www.nairobi.com. Nairobi City Info. (Accessed: 9 January 2015).
http://www.nasa.gov. Fact Sheets: Remote sensing and lasers. (Accessed: 5 January 2015).
http://www.satimagingcorp.com. QuickBird satellite image of the Azadi Tower in Tehran, Iran. (Accessed: 19 January 2015).
http://www.satimagingcorp.com/satellite-sensors/ikonos/. IKONOS Satellite Sensor (0.82m). (Accessed: 6 January 2015).
http://www.satimagingcorp.com/satellite-sensors/other-satellite-sensors/aster/. ASTER Satellite Sensor (15m). (Accessed: 6 January 2015).
http://www.satimagingcorp.com/satellite-sensors/spot-6/. SPOT 6 Satellite Sensor (1.5m). (Accessed: 17 January 2015).
http://www.satimagingcorp.com/satellite-sensors/spot-7/. SPOT-7 Satellite Sensor (1.5m). (Accessed: 17 January 2015).
http://www.science.aster.ersdac.jspacesystems.or.jp/jp/documnts/users_guide/part2/01.html. ASTER Science Project. User Guide. (Accessed: 17 January 2015).
http://www.visitkualalumpur.com. Visit Kuala Lumpur. (Accessed: 20 January 2015).
https://www.cia.gov/library/publications/the-world-factbook/docs/didyouknow.html. CIA.2014. World fact book. (Accessed: 19 January 2015).
https://www.digitalglobe.com. Digital Globe Data Sheet: QuickBird. (Accessed: 29 December 2014).